

# Dendrimers as Carriers for Delivery of Chemotherapeutic Agents

Scott H. Medina and Mohamed E. H. El-Sayed\*

University of Michigan, Department of Biomedical Engineering, 1101 Beal Avenue, Lurie Biomedical Engineering Building, Room 2150, Ann Arbor, Michigan 48109-2110

Received May 4, 2009

## Contents

1. Introduction	3141
2. Dendrimer Families	3141
2.1. PAMAM Dendrimers	3141
2.2. Biodegradable Dendrimers	3143
2.3. Amino Acid-Based Dendrimers	3145
2.4. Glycodendrimers	3145
2.5. Hydrophobic Dendrimers	3146
2.6. Asymmetric Dendrimers	3146
3. Strategies for Synthesis of Dendrimers	3147
3.1. Divergent Synthesis	3147
3.2. Convergent Synthesis	3147
3.3. Combined Convergent–Divergent Synthesis	3148
3.4. “Click” Synthesis	3149
4. Potential of Dendrimers in Cancer Therapy	3149
4.1. Passive Targeting of Dendrimers Therapeutics	3150
4.2. Active Targeting of Dendrimers Therapeutics	3151
5. Mechanisms of Drug Loading onto Dendrimer Carriers	3152
5.1. Physical Encapsulation of Drug Molecules	3152
5.2. Chemical Conjugation of Drug Molecules	3153
5.2.1. Direct Coupling	3153
5.2.2. pH-Sensitive Linkages	3154
6. Conclusions	3154
7. Abbreviations	3155
8. References	3155

## 1. Introduction

Dendrimers are a family of nanosized, three-dimensional polymers characterized by a unique tree-like branching architecture and compact spherical geometry in solution (Figure 1). Their name is derived from the Greek word “dendron”, which means “tree” and refers to the distinctive organization of polymer units. Research into the development of dendrimers started in the 1970s by Vogtle and co-workers, who studied the controlled synthesis of dendritic arms by repetitive reactions of mono- and diamines with a central core to produce polymeric branching units with large molecular cavities.<sup>1</sup> It was not until 1984 that the first family of hyperbranched polymers was developed by Tomalia and his team, who described the iterative coupling of ethylene diamine to a central ammonia core to produce a series of branched macromolecules named “starburst dendrimers”.<sup>2</sup> Dendrimers are composed of individual “wedgies” or dendrons that radiate from a central core where each layer of

concentric branching units constitutes one complete generation (G) in the dendrimer series and is identified with a specific generation number (Figure 1).<sup>3</sup> This branching architecture leads to a controlled incremental increase in a dendrimer’s molecular weight, size, and number of surface groups. Over the past three decades, several synthetic strategies were developed to generate multiple dendrimers families with versatile chemical compositions, which are sought for a variety of applications in chemistry, biology, and medicine.<sup>3–5</sup> This article focuses on the potential of dendrimers as carriers for chemotherapeutic agents for the treatment of cancer. Specifically, we review the different dendrimer families, their synthesis strategies, methods for loading and incorporation of chemotherapeutic agents onto dendritic carriers, and the associated in vitro and in vivo anticancer activity.

## 2. Dendrimer Families

### 2.1. PAMAM Dendrimers

Poly(amidoamine) (PAMAM) dendrimers are the first synthesized and commercialized dendrimers family.<sup>6</sup> Synthesis of PAMAM dendrimers is initiated using an alkyl-diamine core (e.g., ethylene diamine; EDA), which reacts via Michael addition with methyl acrylate monomers to produce a branched intermediate that can be transformed to the smallest generation of PAMAM dendrimers with NH<sub>2</sub>, OH, or COOH surface groups.<sup>2</sup> The reaction of this branched intermediate with excess EDA produces G0 with four NH<sub>2</sub> surface groups. Similarly, the reaction of the same intermediate with ethanolamine produces G0 with four OH surface groups.<sup>7</sup> Hydrolysis of the methyl ester in this intermediate produces the smallest anionic dendrimer (G0.5) with four COOH groups.<sup>2</sup> Synthesis of higher generations of PAMAM dendrimers is achieved by sequential Michael addition of methyl acrylate monomers followed by an exhaustive amidation reaction with EDA (Figure 2). This synthesis method produces highly organized and relatively monodisperse polymers that display a controlled incremental increase in size, molecular weight, and number of surface groups with the increase in generation number (Table 1). However, dendrimers growth eventually reaches a critical point where the steric crowding of the branching arms limits their development into higher generations and possibly produces defective branching architectures in a phenomenon known as the de Gennes dense packing effect.<sup>3</sup> This effect is observed starting with G7, which decreases the synthetic yields of this generation and higher ones until reaching G10, when the synthesis of any larger dendrimers is prohibited by the steric factors.<sup>8</sup>

\* Corresponding author. E-mail: melsayed@umich.edu. Phone: (734) 615-9404. Fax: (734) 647-4834. Web: www.bme.umich.edu/centlab.php.

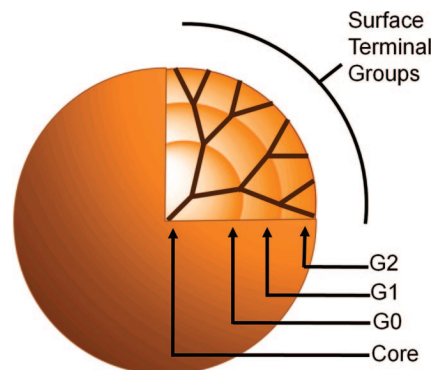


Scott H. Medina was born in Allentown, PA, and received his B.Sc. from Penn State University in 2006. He initiated his graduate studies in the Fall of 2006 with Dr. Mohamed E. H. El-Sayed in the Cellular Engineering and Nano-Therapeutics Laboratory, where his research focuses primarily on the development of novel polymer therapeutics for the treatment of primary hepatic cancer. He completed his M.S. in Biomedical Engineering in 2008 and is presently a doctoral candidate at the University of Michigan, Department of Biomedical Engineering. He is a recipient of the GAANN fellowship for 2006–2007 and 2007–2008 academic years.



Dr. Mohamed E. H. El-Sayed was born in Giza, Egypt, in 1972. He received his Bachelor's degree in Pharmacy & Pharmaceutical Chemistry in May 1994 from Cairo University, Egypt. In 2002, he received his doctoral degree in Pharmaceutical Sciences from the University of Maryland in Baltimore. He subsequently joined the Bioengineering Department at the University of Washington to pursue his postdoctoral training, focusing on the rational design and synthesis of stimuli-sensitive polymers for delivery of macromolecular drugs. Dr. El-Sayed joined the University of Michigan in January 2007 as an Assistant Professor in the Department of Biomedical Engineering, where he established the Cellular Engineering & Nano-Therapeutics Laboratory (CENT LAB). Dr. El-Sayed's research program focuses on the development of optimized drug delivery systems that enhance the therapeutic activity of the incorporated drug while eliminating or minimizing its potential side effects by rationally designing and synthesizing novel polymeric carriers that can effectively "communicate" with the different barriers encountered within the body to selectively deliver their therapeutic cargo to the diseased tissues with cellular and subcellular accuracy. Dr. El-Sayed has received several honors and awards including the Coulter Foundation Translational Research Partnership in Biomedical Engineering Award (2008 and 2009), NSF-Faculty Early Career Development Award (CAREER) (2008), Susan G. Komen Breast Cancer Foundation Postdoctoral Fellowship (2005), U.S. Department of Defense Multidisciplinary Postdoctoral Award (2005), National Cancer Center Postdoctoral Fellowship (2004), University of Maryland School of Pharmacy Academic Merit Award (2001–2002), Charles A. Stevens Memorial Award (2000), and Rho-Chi National Pharmacy Honor Society membership (1999).

The unique chemical architecture of PAMAM dendrimers coupled with their small size has attracted the attention of different groups to explore their applications in biology and

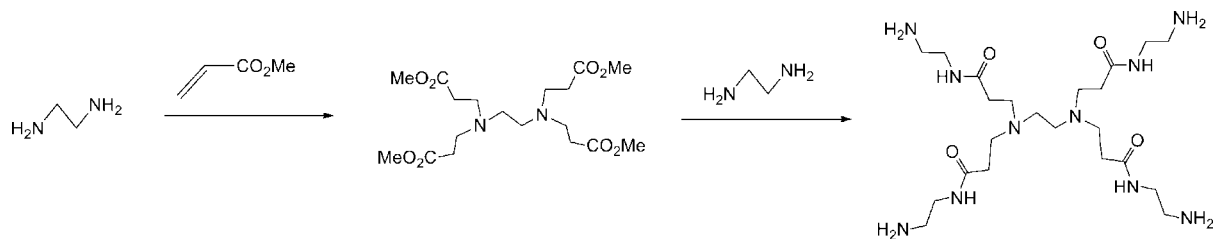


**Figure 1.** Schematic drawing of a G2 dendrimer showing its characteristic treelike branching architecture where each monomer unit is added to a branching point to yield a spherical polymer with a large number of surface groups. Each successive layer of branching units constitutes a new generation (G) with a specific number in the dendrimer series.

medicine, which began by evaluating their toxicity and immunogenicity.<sup>9</sup> Duncan and co-workers reported that G1–G4 of PAMAM–NH<sub>2</sub> dendrimers are cytotoxic upon incubation for 72 h with three different cancer cell lines resulting in IC<sub>50</sub> values ranging from 50–300  $\mu\text{g/mL}$ .<sup>9</sup> Limited morphological changes in B16F10 murine melanoma cells were observed when incubated for 1 h with 5  $\mu\text{g/mL}$  of G4–NH<sub>2</sub> dendrimers, whereas the increase in incubation time to 5 h led to cavities in the cell membrane indicating membrane damage. This damage was attributed to the cationic nature of PAMAM–NH<sub>2</sub> and appeared to be directly related to the generation number, concentration, and incubation time with the cells.<sup>10</sup> This observed toxicity of PAMAM–NH<sub>2</sub> dendrimers decreased dramatically when the free amine surface groups are functionalized with neutral or anionic moieties.<sup>11,12</sup> Partial or full capping of the free NH<sub>2</sub> surface groups using acetic anhydride<sup>13,14</sup> or direct coupling of poly(ethylene glycol) (PEG) chains<sup>15</sup> neutralize the dendrimer's surface, thus reducing its toxicity and improving its solubility. However, these free amine surface groups are essential for enhancing the cytoplasmic delivery of therapeutic molecules via the proton sponge mechanism.<sup>16</sup> Specifically, the internalization and accumulation of PAMAM–NH<sub>2</sub> dendrimers in the endosomes results in protonation of the free amine surface groups as a buffering mechanism, which triggers the diffusion and accumulation of Cl counterions into the endosomes, thus increasing the endosomal osmotic pressure and eventually rupturing the endosomal membrane and releasing its contents, including the loaded dendrimers, into the cytoplasm of the targeted cells.<sup>17</sup>

To maintain the endosomal escape capability of polyamine dendrimers while minimizing their toxicity, Tatu and Jayaraman collaboratively developed G3 poly(ether imine) (PETIM) dendrimers using PEG and PETIM units.<sup>18</sup> Incubation of CV-1 monkey kidney cells with 100 mg/mL of PETIM dendrimers resulted in 98% cell survival, which is a result of dendrimers neutral surface and biocompatible PEG composition. Another group synthesized phosphorus dendrimers (P-dendrimers; G1–G5) possessing a high density of surface amine groups, and these proved to be nontoxic toward 3T3 murine fibroblast cells.<sup>19</sup>

Overall, PAMAM dendrimers are considered ideal carriers for delivery of therapeutic agents including anticancer drugs because of their high aqueous solubility, large number of chemically versatile surface groups, and unique architecture.

**EDA Core****Half Generation****Full Generation**

**Figure 2.** Synthesis of G0–NH<sub>2</sub> as an example for the synthesis of PAMAM dendrimers. Ethylene diamine (EDA) core reacts with methyl acrylate monomers via a Michael addition reaction and yields a branched intermediate (half generation) that reacts with excess EDA to produce the complete G0–NH<sub>2</sub> dendrimer.

**Table 1. Physiochemical Properties of PAMAM–NH<sub>2</sub> Dendrimers (G0–G9) with EDA Core**

generation number	number of surface NH <sub>2</sub> groups <sup>a</sup>	MW <sup>a</sup> (Da)	diameter <sup>a</sup> (nm)
0	4	517	1.4
1	8	1 430	1.9
2	16	3 256	2.6
3	32	6 909	3.6
4	64	14 215	4.4
5	128	28 826	5.7
6	256	58 048	7.2
7	512	116 493	8.8
8	1024	233 383	9.8
9	2048	467 162	11.4

<sup>a</sup> As reported by Tomalia et al.<sup>3</sup>

These distinctive characteristics of PAMAM dendrimers allow for direct conjugation and physical entrapment of anticancer drug molecules to develop dendrimers-based drug delivery systems.<sup>6,20</sup>

## 2.2. Biodegradable Dendrimers

Like all polymer therapeutics, the size and molecular weight of dendrimers-based drug delivery systems dictate their plasma residence time, distribution to tumor tissue, and elimination kinetics.<sup>21–23</sup> The need for biodegradable dendrimers emerged as a strategy to produce the desired large molecular weight carriers that achieve high accumulation and retention in tumor tissue while allowing fast and safe elimination of dendrimer fragments into the urine to avoid nonspecific toxicity. Biodegradable dendrimers are commonly prepared by inclusion of ester groups in the polymer backbone, which will be chemically hydrolyzed and/or enzymatically cleaved by esterases in physiological solutions (Figure 3).<sup>24–27</sup> Grinstaff et al. compared the degradation rate of G1 polyester dendrimers [poly(glycerol–succinic acid); PGLSA] in the presence of acid, base, and esterase enzymes to that of larger G2 polyester–amide and G3 polyester–ether dendrimers to identify the factors that control their degradation kinetics in physiological conditions.<sup>25</sup> Results showed that polyester–ether dendrimers degraded the fastest because of the increased hydrolytic susceptibility of the polyester–ether backbone compared to the polyester and polyester–amide derivatives. Consequently, the following four factors appear to control the rate of degradation of polyester dendrimers: (1) the nature of the chemical bond connecting the monomer units with ester bonds being more susceptible to hydrolysis compared to amide and ether bonds; (2) the hydrophobicity of the monomer units where more hydrophilic polymer units (e.g., glycerol, lactic acid, and succinic acid) result in faster degradation compared to hydrophobic monomers (e.g.,

phenylalanine and alkyl amines); (3) the fact that dendrimers with larger sizes and molecular weights degrade more slowly compared to smaller ones due to the tight packing of their surface, which effectively shields the hydrolyzable bonds; and (4) the cleavage susceptibility of the peripheral and internal dendrimer structure as hydrolysis of the interior linkages leads to faster degradation of the dendrimer structure. Using these established parameters, one can tune the chemical and physical properties of polyester dendrimers to achieve the desired degradation rate for a specific in vivo application.

Because of their biodegradability and biocompatibility, polyester dendrimers have been utilized for delivery of anticancer drugs,<sup>25,28,29</sup> boron neutron capture agents,<sup>29,30</sup> and gene therapy<sup>31–33</sup> for treatment of different cancers. Szoka and Frechet collaboratively reported their pioneering work on the synthesis and biological activity of polyester dendrimers characterized by high water solubility and low toxicity.<sup>21,26,27,34,35</sup> They described the synthesis of polyester dendrimers based on 2,2-bis(hydroxymethyl)propanoic acid<sup>27,35</sup> that were well-tolerated by murine B16F10 carcinoma cells<sup>27</sup> and MDA-MB-231 breast cancer cells<sup>21</sup> upon incubation for 48 h, as well as in vivo when administered as a bolus dose to CD-1 tumor-bearing mice.<sup>27</sup> Szoka and Frechet also reported the synthesis of orthogonal “bow-tie” polyester dendrimers composed of one dendron functionalized with 5–20 kDa PEG chains via degradable carbamate bonds while the other dendron is used for conjugation of drug molecules (Figure 4).<sup>21</sup> Incubation of these bow-tie polyester dendrimers in phosphate (pH 7.4) and acetate (pH 5.0) buffers for 15 days showed that the carbamate linkages were hydrolyzed at both pH values, whereas the ester groups present in the polymer backbone were hydrolyzed only at pH 7.4 and dominated the degradation pathway in mildly basic conditions (pH 9.0).<sup>21</sup> Results also showed that the steric hindrance of the ester linkages within the bow-tie dendrimers resulted in slow degradation rates of the dendrimer’s backbone, which took months to be completely degraded. This slow degradation profile of the bow-tie dendrimers enhances their stability along with the loaded anticancer drugs in the systemic circulation; however, it also leads to poor filtration of the dendritic carriers into the urine and can possibly induce nonspecific toxicity. Overall, polyester dendrimers have attracted a lot of attention because of their biocompatibility both in vitro and in vivo, as well as degradability under physiologic conditions. However, their nonspecific hydrolysis mechanism and long degradation time have prompted the search for novel biodegradable dendrimers designed to achieve specific spatial and temporal degradation profiles.



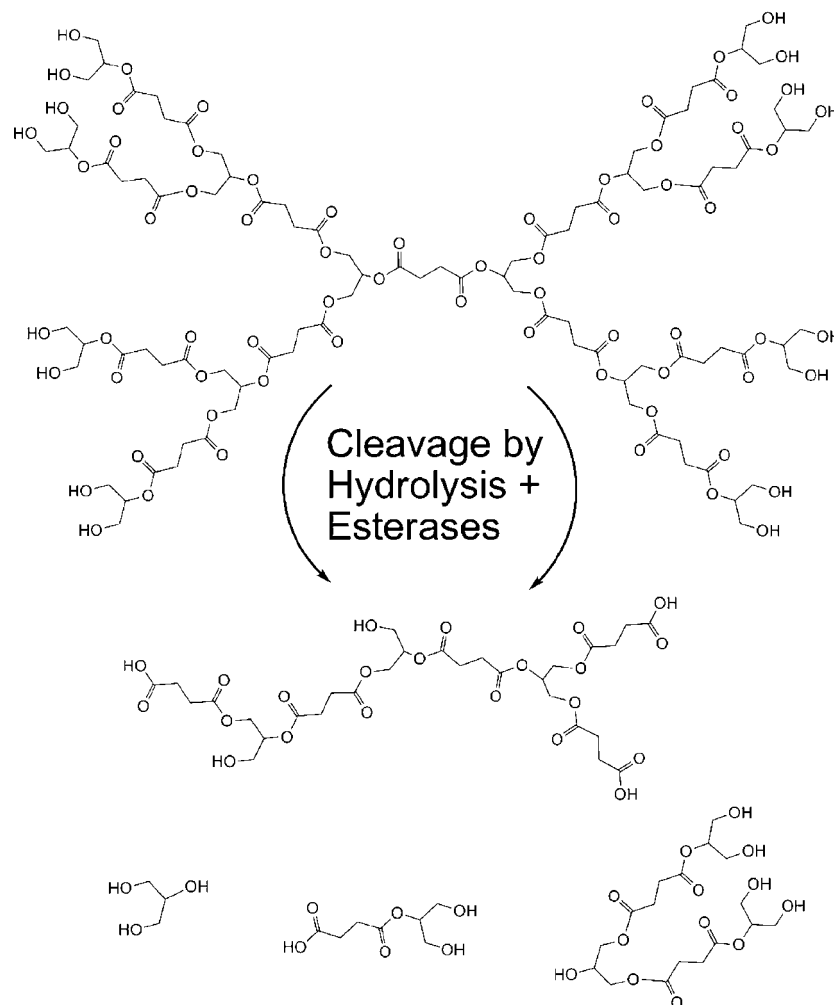


**Figure 3.** Cleavage of a polyester dendrimer by hydrolysis and tissue esterases. Degradation reduces the dendrimers to small molecular weight polymer units that are rapidly secreted into the urine to minimize exposure time-dependent carrier toxicity.

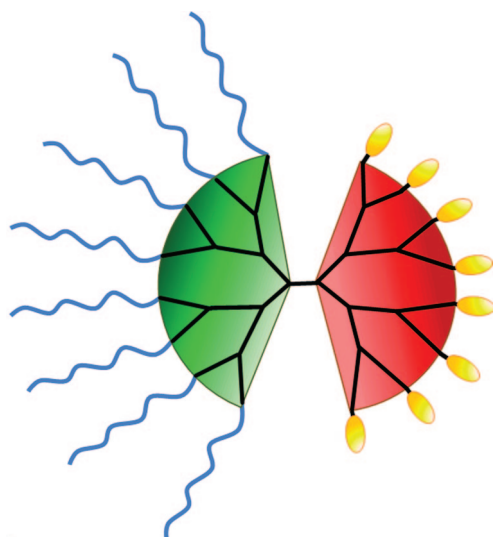


**Figure 4.** Diagram of “bow-tie” polyester dendrimers reported by Szoka and Frechet.<sup>21</sup> The left dendron (green) is functionalized with 5–20 kDa PEG arms (blue lines) via degradable carbamate linkages to increase the dendrimers plasma half-life, whereas the orthogonal dendron (red) is used for loading of anticancer drug molecules (yellow ovals).

Another class of polyester dendrimers was synthesized from dimeric and tetrameric hydroxybutanoic (HB) acid monomers producing an enzyme-sensitive family of den-

drimers that can be hydrolyzed by a bacterial depolymerase isolated from *A. faecalis*, named PHB-depolymerase (Figure 5).<sup>36</sup> Incubation of these dendrimers with the PHB-depolymerase enzyme resulted in a nearly 100 times faster degradation of the tetrameric dendrimers compared to the dimeric derivatives. This work showed the feasibility of developing enzyme-sensitive biodegradable polyester dendrimers.

Recently, Ou and co-workers developed poly(disulfide amine) dendrimers with well-defined sites for enzymatic cleavage embedded in the polymer backbone.<sup>31</sup> Disulfide linkages were selected due to their improved hydrolytic stability at physiologic pH values (pH 7.4) compared to ester linkages while allowing selective reduction by intracellular glutathione and thioredoxin reductase enzymes into the corresponding SH groups. These dendrimers selectively released their therapeutic cargo upon incubation with dithiothreitol, which reduced the disulfide linkages in the polymer's backbone, thus degrading the dendrimers structure that mimics intracellular reductases. Biodegradable dendrimers with acid-sensitive branching points were explored by Kohman et al., who reacted alkyne-functionalized monomer units to a triazide core via “click” chemistry.<sup>37</sup> Addition of HCl to a solution of these “clicked” dendrimers proved to degrade the polymer backbone at the polymer's acid-sensitive focal/branching points.<sup>37</sup>

Shabat and co-workers developed another class of degradable dendrimers, where they used the substrate of 38C2

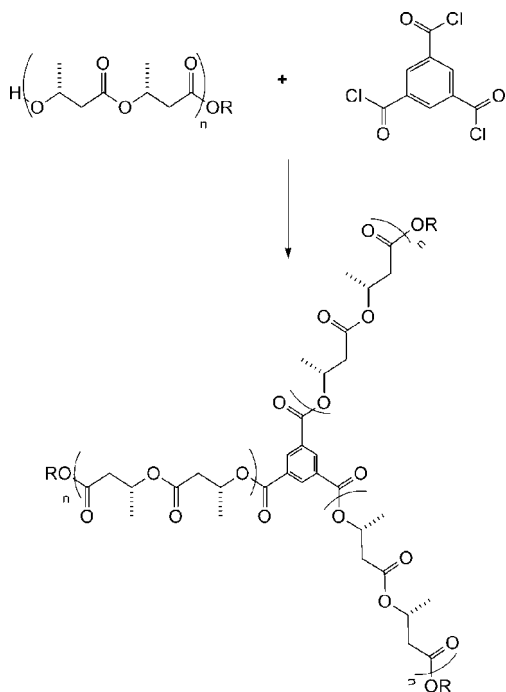


**Figure 5.** Synthesis of hydroxybutanoic (HB) acid based dendrimers where dimeric ( $n = 1$ ) or tetrameric ( $n = 2$ ) HB units are coupled to a trimesic acid trichloride core. Successive generations of these dendrimers are synthesized by iterative coupling of dibranched HB units to produce up to G2 dendrimers, which are hydrolyzed by the PHB-depolymerase enzyme via hydrolysis of ester linkages.<sup>36</sup>

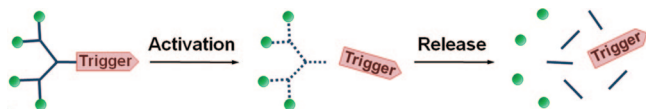


**Figure 6.** Schematic drawing showing the mechanism of release of CPT and DOX anticancer drugs conjugated to self-eliminating dendritic carriers. Specifically, the binding of 38C2 antibody to its substrate triggers a sequence of retro-aldol, retro-Michael cleavage reactions, which consequently result in self-elimination of the spacer and release of the attached drug molecules.<sup>38</sup>

catalytic antibody as the core of the dendrimer structure and attached camptothecin (CPT) and/or doxorubicin (DOX) anticancer drugs to the dendrimer surface groups via a self-eliminating spacer.<sup>38</sup> Binding of the 38C2 antibody to its substrate triggers a sequence of retro-aldol, retro-Michael cleavage reactions, which result in a series of self-eliminating reactions of the spacer and release of the attached drug molecules (Figure 6). These self-eliminating dendritic prodrugs were approximately 40 times more toxic in the presence of the triggering agent, 38C2 antibody, against human MOLT-3 cells.<sup>38</sup>

### 2.3. Amino Acid-Based Dendrimers

Amino acid-based dendrimers were developed to capitalize on the unique properties of the amino acid building blocks including chirality, hydrophilicity/hydrophobicity, biorecognition, and optical properties. For example, chirality of amino acid-based dendrimers is a product of the chirality of the core, branching units, and terminal surface groups, which influence the arrangement of the surface groups and the overall shape of the dendrimer. Optically active protein-mimetic dendrimers have been synthesized using a library of amino acids including tryptophane,<sup>39</sup> phenylalanine,<sup>40</sup> glutamic acid,<sup>40,41</sup> aspartic acid,<sup>41</sup> leucine,<sup>42,43</sup> valine,<sup>42,43</sup>

glycine,<sup>43</sup> and alanine.<sup>43</sup> The distinctive internal composition created by the amino acid building blocks offers stereoselective sites for noncovalent interactions with guest/drug molecules. In addition, the unique structural folding of the branching units has yielded a number of chiral dendrimers with applications as protein mimetics,<sup>44–46</sup> carriers for gene therapy,<sup>47–50</sup> and targeted drug delivery systems.<sup>51–53</sup>

Amino acid-based dendrimers are synthesized using one of the following strategies: (1) amino acid or peptide grafting and display on the surface of a conventional dendrimer or (2) attachment of amino acids or peptides to an organic or peptide core.<sup>54,55</sup> Newkome described one of the first amino acid functionalized dendrimers, which was synthesized by grafting tryptophane to the surface of poly(ether amide) dendrimers to modulate the encapsulation of hydrophobic molecules into the voids of the dendritic carrier.<sup>39</sup> Similarly, Kono et al. studied the retention of Rose Bengal dye in PEGylated (2 kDa PEG chains) G4-NH<sub>2</sub> dendrimers with phenylalanine and glutamate amino acids grafted to the dendrimer's surface groups.<sup>40</sup> Using the Klotz plot, Kono found that the hydrophobic amino acid layer displayed on the dendrimer's surface resulted in a 10-fold increase in the binding affinity of hydrophobic dye molecules to the amino acid-functionalized dendrimers compared to nonfunctionalized ones. Results show that grafting of the phenylalanine to the surface of PAMAM dendrimers modulate their aqueous solubility in a thermally responsive fashion.<sup>56</sup> It is interesting to note that dendritic polylysine proved to be more effective in delivering therapeutic nucleic acids into cancer cells compared to the linear counterpart while displaying significantly lower cytotoxicity.<sup>49,57</sup>

### 2.4. Glycodendrimers

Carbohydrate interactions with different receptors displayed at the cell surface control a number of normal (e.g., lymphocyte activation and cell–cell adhesion) and abnormal (e.g., cell–pathogen adhesion and cancer cell metastasis) biological processes. The affinity of carbohydrate–receptor interactions is typically low for a single carbohydrate ligand but has been shown to increase significantly through multivalent ligand–receptor interactions, which result in clustering and cross-linkage of the displayed receptors.<sup>58,59</sup> Consequently, several research groups have attempted to develop well-defined macromolecules displaying a large number of carbohydrate ligands using dendrimers as carriers to achieve multivalent carbohydrate–receptor interactions and utilize them for recognition and targeting to specific cells.

Okada's group described the synthesis of “sugar balls” where they functionalized the surface groups of G2–G4 PAMAM dendrimers with lactose and maltose sugars (Figure 7).<sup>60</sup> These glycodendrimers retained the binding specificity of the attached sugars confirmed by the ability of PAMAM–maltose conjugates to precipitate concanavalin A, which is a lectin that selectively recognizes and binds the maltose sugar.<sup>60</sup> Okada's group expanded the library of the sugars used to develop the sugar balls by grafting  $\alpha$ -amino acid derivatives, *N*-carboxyanhydride (glycoNCA) glucose and *N*-acetyl-D-glucosamine ligands, onto the surface of PAMAM carriers.<sup>61,62</sup>

Other glycodendrimers have been synthesized by coupling isothiocyanate functionalized glycosyl<sup>63</sup> and mannopyranoside<sup>64</sup> ligands as well as an *N*-hydroxysuccinimide (NHS) activated galactopyranosyl derivative<sup>65</sup> to amine-terminated dendrimers. Furthermore, research into dendritic glycosides

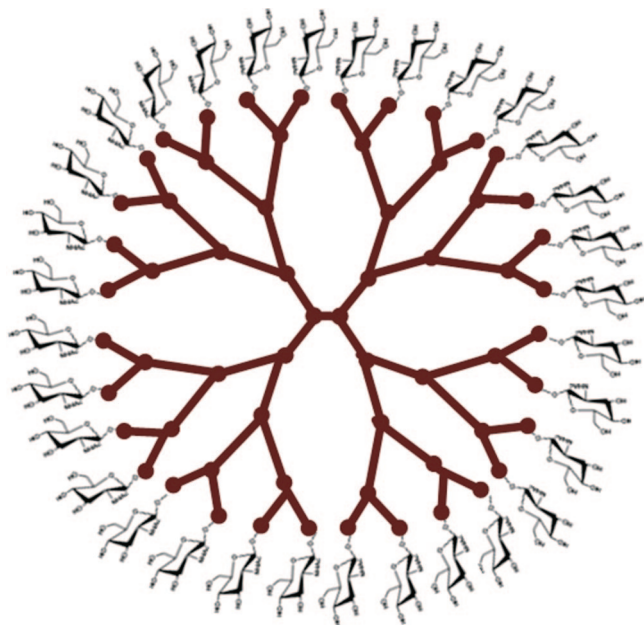


**Figure 7.** Drawing of the “sugar balls” developed by Okada and co-workers, which are composed of glycoNCA sugar molecules displayed on the surface of a PAMAM carrier.<sup>60</sup>

has produced carbohydrate terminated dendrons, which afford increased contact and interaction of the conjugated carbohydrates (e.g., glycosides) with target receptors (e.g., hemeagglutinins) due to the compact geometry of the dendron carrier.<sup>66</sup> Coupling of functionalized glycodendrons to a central core has created highly organized multivalent glycodendrimers, which can serve as efficient targeting agents for cell-specific localization. For example, Roy et al. synthesized a number of  $\alpha$ -sialoside-functionalized glycodendrons as a multivalent inhibitor of influenza,<sup>67,68</sup> which opened the door for development of several new glycodendrons for treatment of viral infections.<sup>59,66</sup>

Another application of glycodendrimers in cancer therapy is the use of sugar-functionalized dendrons to stimulate the immune response against cancer cells.<sup>69</sup> Specifically, Nakahara and co-workers produced octameric glycopeptide dendrimers by conjugating a Gal–GalNAc dimer to a trimeric lysine peptide to serve as a cancer vaccine where the Gal–GalNAc groups displayed on the dendrimer surface mimic the sugar expressed in the mucins of several adenocarcinomas and consequently trigger the production of the corresponding antibody.<sup>69</sup> Similarly, Andre et al. synthesized lactose terminated G1–G3 dendrons based on 3,5-di-(2-aminoethoxy)benzoic acid units to act as antimetastatic agents by inhibiting lectin-mediated cell adhesion.<sup>70</sup> Results showed that glycodendrons inhibited lectin binding to immobilized glycoproteins, and the affinity of sugar–lectin interactions depends on both glycoside valency and conformational matching of the carbohydrate ligand with the lectin binding site.<sup>70</sup> These studies clearly demonstrate the potential of glycodendrimers in cancer therapy not only as targeted carriers for chemotherapeutic agents but also as antimetastatic agents and stimulants for the immune system.

## 2.5. Hydrophobic Dendrimers

Dendrimer-based drug delivery systems should be water-soluble to facilitate their systemic administration. However, the inclusion of hydrophobic regions in the dendrimer structure allows for better encapsulation and efficient solu-

bilization of hydrophobic drug molecules within the dendrimer voids. Specifically, dendrimers with hydrophobic cores proved to effectively retain hydrophobic drug molecules in the voids of their branching architecture, mimicking amphiphilic polymer micelles.<sup>71,72</sup> However, unlike polymeric micelles, which require a specific “critical micelle concentration” to remain intact in solution, dendrimers building units are covalently bound and do not dissociate in diluted solutions. Newkome and co-workers capitalized on this concept and developed unimolecular micelles using dendrimers with hydrophobic interiors and a hydrophilic surface, which were used to solubilize and encapsulate hydrophobic guest molecules including lipophilic probes (e.g., diphenyl-hexatriene), dyes (e.g., pinacyanol chloride), and fluorescent markers (e.g., chlortetracycline).<sup>73</sup> The same concept was used by the Diederich research group to develop dendritic cyclophanes or “dendrophanes” to encapsulate aliphatic and aromatic moieties and study their inclusion kinetics.<sup>74</sup> Frechet and co-workers have also developed new amphiphilic dendrimers starting with the hydrophobic 4,4-bis(4'-hydroxyphenyl) pentanol monomer to develop a nonpolar dendritic scaffold, which was coupled to PEG chains (750 Da) to develop unimolecular micelles that successfully encapsulated the hydrophobic pyrene molecules and increased its aqueous solubility by 365-fold.<sup>72,75</sup> These micelles also proved to decrease the release rate of the encapsulated indomethacin drug molecules by 6-fold.<sup>72,75</sup>

## 2.6. Asymmetric Dendrimers

Symmetry of dendrimer's architecture is a result of the controlled iterative synthetic steps, which produces highly monodisperse and symmetrical polymers. However, imparting asymmetry to dendrimer's architecture can provide a range of novel structures, which may favorably affect their pharmacokinetic profile in vivo. Asymmetric dendrimers are synthesized by coupling dendrons of different generations to a linear core, which yields a branched dendrimer with a nonuniform orthogonal architecture. This asymmetry allows for tunable structures and molecular weights, with precise control over the number of functional groups available on each dendron for attachment of drugs, imaging agents, and other therapeutic moieties. The most recognized asymmetric dendrimers were synthesized by Frechet and co-workers and are known as the “bow-tie” polyester dendrimers (Figure 4).<sup>21,76</sup> These bow-tie dendrimers are based on 2,2-bis(hydroxymethyl)propionic acid and carry dendrons of different generations (G1–G3) with variable degrees of PEGylation (2–8 PEG arms, each is 1–20 kDa), which produced well-defined dendrimers with tunable molecular weights of 2–160 kDa.<sup>76</sup> Subsequent studies showed that G1–G3 bow-tie dendrimers functionalized with 5, 10, and 20 kDa PEG arms were nontoxic to MDA-MB-231 breast cancer cells upon incubation for 48 h.<sup>21</sup> Furthermore, biodistribution studies of these bow-tie dendrimers in CD-1 female mice bearing B16F10 tumors showed that varying the generation number/size of the incorporated dendron and the number and molecular weight of the attached PEG arms influenced the plasma half-life of these asymmetric dendrimers ranging from 1.4–50 h and resulted in accumulations of ~15% of the injected dose per gram of tumor tissue for the largest asymmetric carrier. Another class of asymmetric dendrimers was developed by Lee and co-workers who utilized “click” chemistry to couple a propargyl G4 dendron to an azide-functionalized G3 dendron, forming a triazole core.<sup>77</sup> While



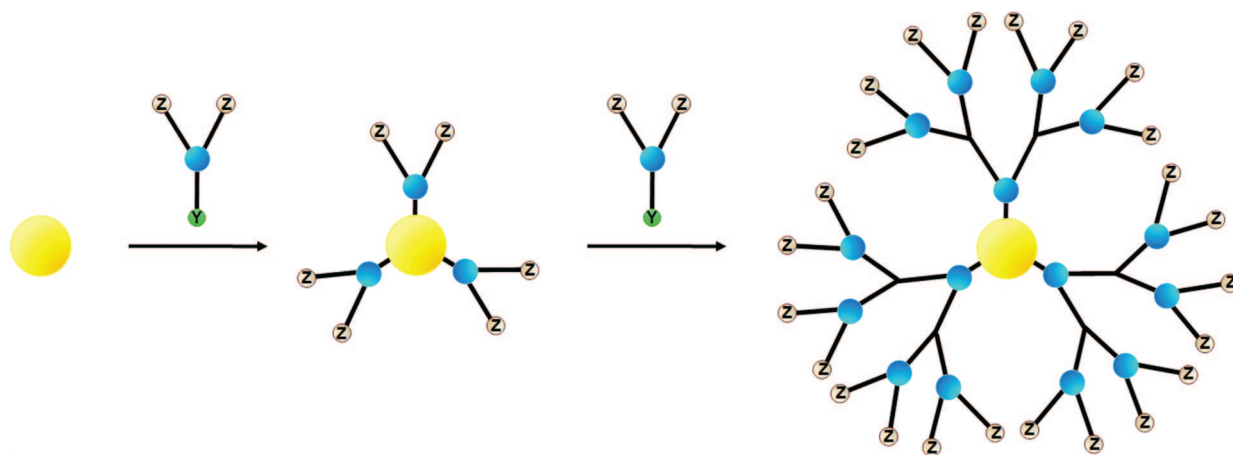


**Figure 8.** Schematic drawing showing the divergent method for synthesis of dendrimers. It starts with a multifunctional initiator core (yellow) that reacts with the chemically activated focal point (Y) of a branched monomer (blue) to produce the first-generation dendrimer. Higher generations are synthesized by the iterative addition of the branched monomers, producing a complete dendrimer terminated with functional chemical groups (Z).

limited biological studies have been done using these “clicked” asymmetric dendrimers, their application in cancer therapy is clear since they have the potential for bifunctional derivatization where one dendron can be functionalized with PEG chains or targeting moieties to improve the net biocompatibility and enhance cell-specific localization while the orthogonal dendron can be loaded with the desired therapeutic cargo.

### 3. Strategies for Synthesis of Dendrimers

#### 3.1. Divergent Synthesis

Divergent dendrimer synthesis is a technique that effectively grows the dendrimer structure from the initiator core to the periphery in a stepwise fashion by iterative addition of monomer units. Specifically, divergent synthesis is initiated by coupling of a monomer unit to a multifunctional initiator core where the dendrimer generation increases by successive addition of the building blocks to the surface of the parent dendrimer (Figure 8). Tomalia and co-workers used this strategy to couple *N*-(2-aminoethyl)acrylamide monomers to an ammonia core to develop PAMAM-NH<sub>2</sub> dendrimers.<sup>2</sup> Each branching unit is synthesized in a two-step sequence starting with exhaustive Michael addition of the acrylate ester to the ammonia core followed by amidation with excess EDA. The first step produces a half-generation, and the addition of the diamine yields the full generation. This synthesis strategy can be hindered by side reactions that yield incomplete or imperfect dendrimers. For example, an incomplete Michael addition reaction leaves a fraction of the surface amine groups free and subject to intramolecular cyclization reactions and fusion of the growing branches.<sup>2</sup> Dendrimer degradation via retro-Michael addition reaction is also a concern at high reaction temperatures (>80 °C), which leads to dendrimer fragmentation. In addition, hydrolysis of the methyl ester group occurs rapidly in aqueous solutions and yields carboxylic acid groups, which are not reactive toward amines under Tomalia’s reaction conditions, thus blocking the formation of complete generations.<sup>2</sup> Large molar excess of reagents is used to limit these undesirable side reactions along with careful removal of the unwanted byproducts after each step to avoid side reactions in any subsequent step.

PAMAM dendrimers are the first class of dendrimers that were systematically synthesized, characterized, and commercialized using the divergent synthesis strategy.<sup>6</sup> However, divergent synthesis has its own limitations besides nonideal growth events, including the difficulty in purifying the final product from structurally similar byproducts and the lengthy multistep reactions, which led to a number of optimizations. For example, Frechet and co-workers described the divergent synthesis of an aliphatic ester dendrimer, which utilized anhydride coupling to reduce the purification steps to simple extraction and precipitation.<sup>78</sup> Specifically, protected 2,2-bis(hydroxymethyl)propionic acid is coupled using dicyclohexylcarbodiimide (DCC) to form an orthogonal anhydride derivative. Subsequently, the purified anhydride is coupled to 1,1,1-tris(hydroxyphenyl)ethane core by esterification. This process yielded high-purity compounds, since simple extraction and precipitation could be used during each step of synthesis, and produced dendrimers as high as G6. Another improvement involves the use of branched monomeric building blocks, which allow direct grafting of different branching sections to form a complete dendritic scaffold.<sup>79,80</sup> For example, Maraval et al. described the synthesis and coupling of two dendritic building blocks, a branched azide diamine and a diphosphine alcohol labeled as CA<sub>2</sub> and DB<sub>2</sub>, respectively.<sup>79</sup> G1 dendrimers were synthesized by coupling 3 equiv of the CA<sub>2</sub> azide functionalized monomers to a triphosphine (B<sub>3</sub>) core, which after purification is followed by condensation of the DB<sub>2</sub> monomer to produce a G2 phosphine terminated dendrimer. The successive addition of the CA<sub>2</sub> and DB<sub>2</sub> blocks yields higher generation dendrimers.

#### 3.2. Convergent Synthesis

The convergent approach to dendrimer synthesis was developed to address the deficiencies of the divergent method. Convergent synthesis begins with the dendrimer surface units coupled to additional building blocks to form the branching structure, thus constructing dendrons from the periphery toward the central focal point (Figure 9). Each dendron is then coupled through its focal point to a multifunctional core to produce the complete dendrimer. Unlike divergent synthesis, convergent reactions are simple to purify since the desired dendrons are substantially different

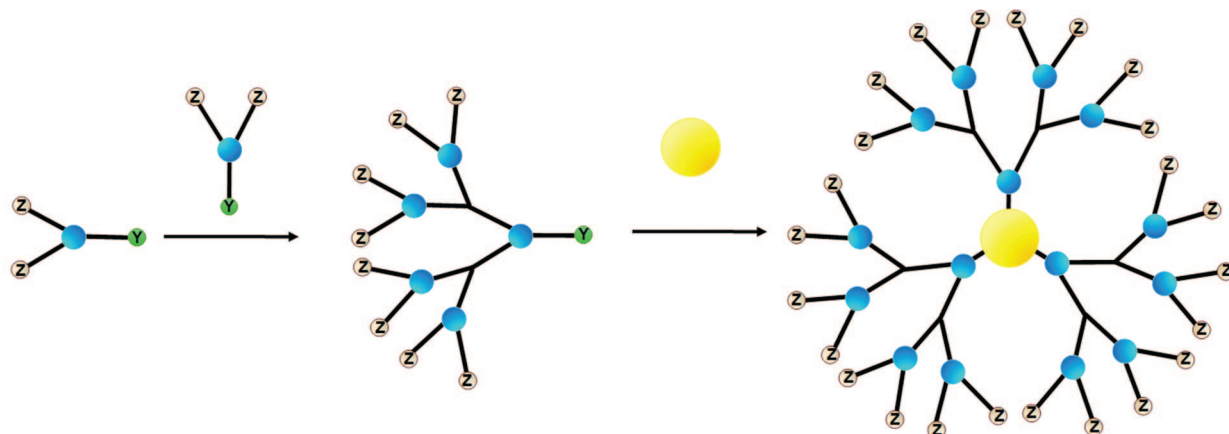


**Figure 9.** Schematic drawing showing the convergent method for synthesis of dendrimers. The dendrimer surface is formed by reaction of the chemically active focal point (Y) of the branched monomer to the functional groups (Z) of another monomer. Dendrons grow by iterative coupling of monomer units to the parent dendron until the desirable dendron size is reached followed by coupling the dendron's focal point to a multifunctional initiator core (yellow) to produce the complete dendrimer.

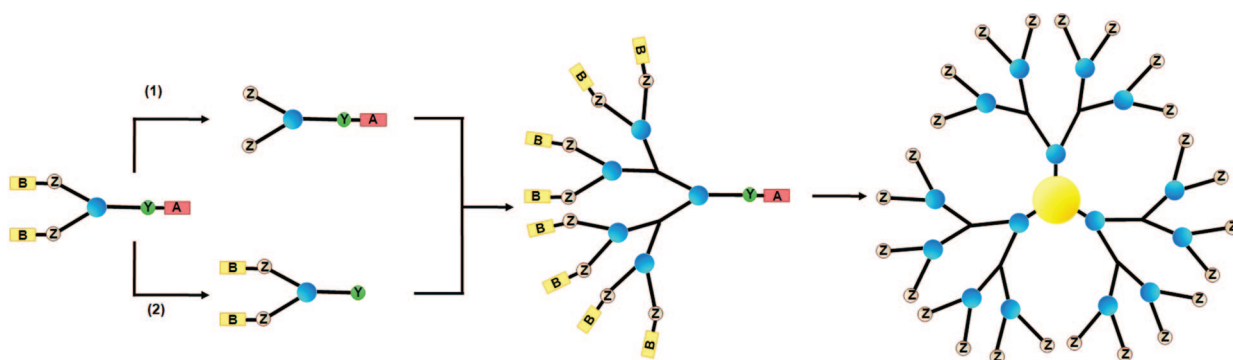


**Figure 10.** Schematic drawing showing the convergent-divergent method for dendrimer synthesis. In this method, the branched monomer is protected at the focal point (Y) with protection group A and at the terminal groups (Z) with protection group B. Using separate deprotection schemes, the monomer's terminal groups (1) or the focal point (2) are deprotected and coupled together to yield the dually protected dendron. Divergent dendron growth can then continue through deprotection of B and iterative monomer coupling or the complete dendrimer can be formed by deprotection of A and coupling of the dendron focal point (Y) to a multifunctional core followed by deprotection of B.

from the reaction byproducts, thus eliminating the need for highly efficient reactions. While the number of synthetic steps is similar for both convergent and divergent techniques, the convergent approach has fewer nonideal growth events, which leads to improved monodispersity of the final dendrimers.

In 1990, Hawker and Frechet collaboratively published a convergent method to synthesize polyether dendrimers based on 3,5-dihydroxybenzyl alcohol units coupled to an activated benzyl bromide to afford successive dendron generations.<sup>81</sup> In their report, 3 equiv of the bromine activated dendrons reacted with a triphenolic core to produce G3–G6 dendrimers, which were found to be highly monodisperse (polydispersity index = 1.01–1.02). However, the increase in dendrimer's generation reduced the synthetic yields from 84% for G4 to 51% for G6, which is a result of steric crowding that lowered the reactivity of dendrons focal point. Furthermore, chromatographic characterization during the construction of convergent dendrons became increasingly difficult with larger generations since the monomer addition does not produce a significant increase in the product's molecular weight relative to the parent dendron.

Subsequently, Frechet proposed what is called a “double-staged” approach to increase synthetic yields of higher-generation dendrimers by coupling dendrons prepared by convergent synthesis to a dendrimer “hypercore” or a

prefabricated lower-generation dendrimer utilized as a multifunctional core.<sup>82</sup> This method allows the use of a dendrimer hypercore that is constructed from flexible units to reduce the steric hindrance during the coupling of the dendron focal points. For example, flexible 4,4-bis(4'-hydroxyphenyl)pentanol monomers were used as a dendrimer hypercore, prepared by convergent synthesis up to G2 using bromine activation.<sup>82</sup> G4-bromide dendrons synthesized in Frechet's previous study<sup>81</sup> were then grafted onto the carboxyl-terminated G2 hypercore, producing a G6 dendrimer with a 61% yield after purification, which is an improvement over the 51% yield obtained with the single-stage convergent method. It is important to note that large hypercores impart flexibility, which allows folding of the dendritic arms toward the core, thus yielding dendrimers with oblong geometries and diverse internal void architectures.

### 3.3. Combined Convergent–Divergent Synthesis

Kawaguchi et al. described a hybrid convergent–divergent synthesis called “double exponential growth” to further accelerate dendrimer synthesis by using orthogonally protected branched monomers with protecting groups that are stable during cleavage of the opposing functionality (Figure 10).<sup>83</sup> The approach begins with selective deprotection of the branched monomer surface groups to produce an



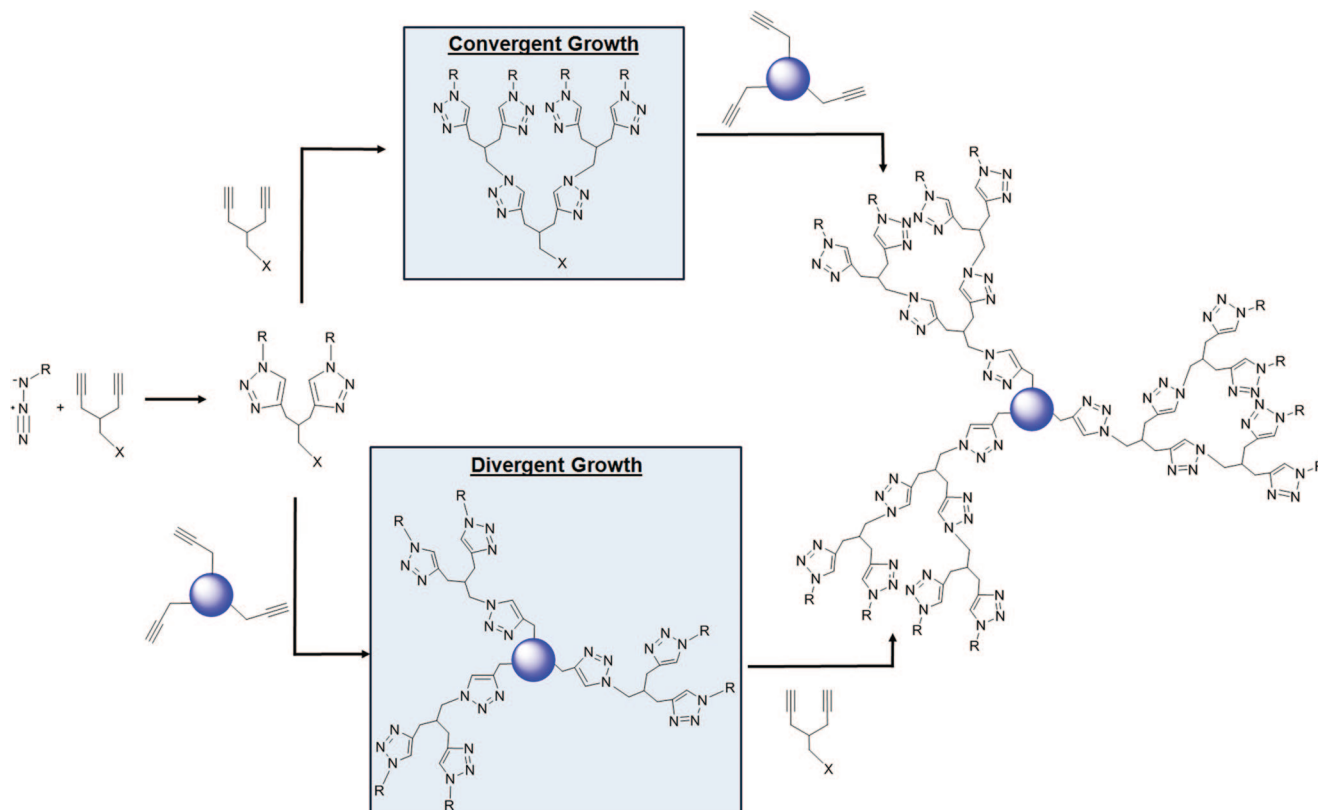


**Figure 11.** Diagram showing the synthesis of “clicked” dendrimers based on the branched monomer described by Hawker and Frechet.<sup>85,86</sup> The monomer is prepared by coupling of a functional azide ( $R-N_3$ ) to a branched alkyne ( $[C\equiv C]_2-X$ ), producing the branched triazole building block. Convergent dendron growth is accomplished by coupling of the branched alkyne to the monomer functional groups ( $R$ ) followed by reaction with the azide to increase the dendron generation. The dendron focal point ( $X$ ) is converted to an azide and coupled to a trialkyne core to produce the complete dendrimer. Divergent growth begins with conversion of the monomer focal point ( $X$ ) to an azide, which is coupled to the trialkyne core. Iterative reaction of terminal functional groups ( $R$ ) to the branched alkyne followed by “click” coupling of the azide moiety results in the growth of the divergent clicked dendrimers.

activated convergent monomer or deprotection of the focal point resulting in a divergent monomer. Coupling of these products gave the first-generation dendrimer by the divergent approach. The parent dendron can then be exponentially grown by coupling to an activated dendron, where each additional activation and coupling sequence doubles the final dendron generation. The complete dendrimer can then be prepared by coupling of the activated dendrons to a central core.

Kawaguchi's first report on the application of this double exponential growth technique described the synthesis of phenylacetylene dendrimers utilizing a tribranched phenyl monomer with a triazene protected focal point and two orthogonal trimethylsilyl (TMS)-protected alkynes.<sup>83</sup> Two equivalents of the deprotected first-generation TMS dendron were coupled to an iodo-activated first-generation dendrimer to produce the second-generation dendrimer. Subsequent activation, deprotection, and coupling steps produced the fourth-generation dendrimer, but synthesis of higher generations was not possible due to incomplete reactions as a result of the steric hindrance. While the double exponential growth technique combines the advantages of both convergent and divergent approaches to rapidly assemble dendrimers, it also suffers from their combined disadvantages. Specifically, protection and activation chemistry increases exponentially with generation, requiring highly efficient reaction schemes. In addition, because the dendrimer size is doubled at each coupling step, there are a limited number of generations that can be created before significant steric hindrance is encountered.

### 3.4. “Click” Synthesis

“Click” chemistry refers to Cu-catalyzed cycloaddition reaction of an alkyne and an azide to form a 1,2,3-triazole ring. The coupling specificity, mild reaction conditions, and quantitative synthetic yields of click reactions motivated the synthesis of dendrimers using this method.<sup>84</sup> G3 triazole dendrimers were synthesized using a branched alkyne monomer with an alkyl chloride focal point.<sup>85,86</sup> Using the convergent approach, dendrons are synthesized by triazole formation with the peripheral monomer alkynes followed by conversion of the focal point to an azide functionality for reiterative monomer addition (Figure 11). Coupling of the dendrons to a polyacetylene core produced G3 triazole dendrimers with a 92% yield after simple aqueous workup and filtration to remove the NaCl byproduct.<sup>85,86</sup> It is important to note that “clicked” dendrons can be used to produce symmetric<sup>87</sup> and asymmetric PAMAM<sup>77</sup> dendrimers, which increases their chemical and architectural versatility.

## 4. Potential of Dendrimers in Cancer Therapy

Dendrimers are particularly well-suited for the delivery of anticancer drugs and imaging agents<sup>4,88,89</sup> because of their high water solubility,<sup>90–92</sup> monodisperse size, and uniform composition,<sup>93</sup> which will lead to consistent batch-to-batch anticancer activity of dendrimers-based drug delivery systems.<sup>94</sup> In addition, dendrimer's unique branching architecture and high number of functional groups present on the surface can be utilized to either encapsulate<sup>95</sup> or directly conjugate<sup>88,96</sup>

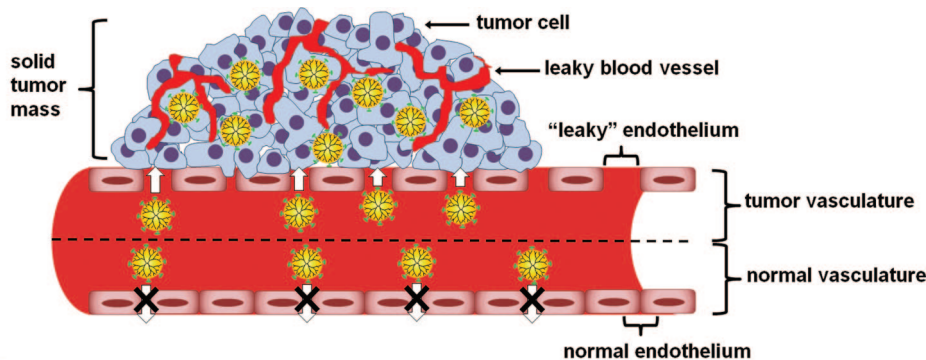


**Figure 12.** Illustration showing the diffusion of dendrimers-based drug delivery systems (yellow) across the tumor's leaky vasculature into the tumor tissue and their retention due to the impaired lymphatic drainage, which is a phenomenon known as the enhanced permeability and retention (EPR) effect.

large payloads of therapeutic molecules that will be shuttled to the cytoplasm of cancer cells.<sup>48,97</sup> Cellular uptake of dendrimers-based drug delivery systems proved to be significantly higher than linear polymeric carriers such as *N*-(2-hydroxypropyl)methacrylamide (HPMA)<sup>98–100</sup> and PEG,<sup>101,102</sup> which can be attributed to dendrimer's nano size and compact spherical geometry in solution. For example, Jelinkova et al. compared the toxic effect of antibody-targeted, linear and branched HPMA–DOX conjugates on T-cell lymphoma and human colorectal carcinoma cell lines.<sup>98</sup> Branched HPMA polymers incorporated an equal weight % of DOX at approximately half the molecular weight of the linear HPMA carrier while simultaneously displaying 1.5–2-fold the weight % of the targeting antibody. These branched HPMA–DOX conjugates were 3–11-fold more toxic toward both cancer cell lines compared to the linear HPMA–DOX conjugates.<sup>98</sup> Furthermore, branched HPMA–DOX conjugates produced a significant increase in the plasma residence time of the incorporated DOX molecules compared to linear HPMA–DOX conjugates at late time points (12–48 h) after a single intravenous injection of each conjugate into male Balb/c mice.<sup>98</sup> Another study by Minko and co-workers compared the anticancer activity of G4–paclitaxel (TAX) conjugates to linear PEG–TAX carrying an equal amount of TAX against ovarian cancer cells, which showed that G4–TAX conjugates were 10-fold more toxic compared to free TAX whereas PEG–TAX conjugates were 25-fold less toxic than the free drug.<sup>101</sup> Minko and co-workers also compared the anticancer activity of peptide-targeted stealth liposomes encapsulating an equal amount of TAX to that incorporated in targeted G4–TAX and targeted linear PEG–TAX conjugates against human lung cancer cells.<sup>103</sup> These three formulations showed similar in vitro cytotoxic effect and reduced the tumor size in vivo. However, G4–TAX conjugates displayed the highest tumor-to-liver accumulation ratio, which indicate their preferential distribution to tumor tissue and the ability to escape recognition by the reticular endothelial system (RES). In addition, the covalent bonding of dendrimer's building blocks yields a more stable carrier that withstands physiological conditions compared to liposomes and amphiphilic particles, which undergo rapid dissociation, causing a quick and nonspecific drug release.<sup>104,105</sup> Dendritic carriers have also been shown to improve the therapeutic activity of the incorporated anticancer drugs against resistant cancer cells.<sup>106,107</sup> For example, one study compared the anticancer activity of the drug Methotrexate (MTX) when conjugated to a dendrimer carrier on sensitive and resistant human acute lymphoblastoid leukemia cells, which showed that dendrimer–MTX con-

jugates are 8-fold more toxic toward resistant cells than free MTX drug at similar concentrations.<sup>107</sup> These studies clearly indicate that dendrimers-based drug delivery systems are more effective in delivering anticancer drugs compared to their linear counterparts due to favorable internalization kinetics and efficient escape into the cytoplasm of the targeted cells.

#### 4.1. Passive Targeting of Dendrimers Therapeutics

Therapeutic macromolecules including dendrimers-based drug delivery systems exploit the pathophysiological patterns of solid tumors, particularly their leaky vasculature, to preferentially extravasate and accumulate in tumor tissue in a process known as the enhanced permeability and retention (EPR) effect (Figure 12).<sup>108</sup> The amount of dendrimers-based drug delivery systems that accumulates in tumor tissue is influenced by their size, molecular weight, and surface charge, which affect their residence time in the systemic circulation, transport across the endothelial barrier, and nonspecific recognition and uptake by RES.<sup>109</sup> El-Sayed et al. studied the effect of size, molecular weight, and surface charge on the permeability of fluorescently labeled PAMAM–NH<sub>2</sub> (G0–G4) dendrimers across epithelial and endothelial barriers.<sup>10,110–112</sup> Their data showed that the increase in dendrimers size/molecular weight results in a corresponding exponential increase in their extravasation time ( $\tau$ ) across the microvascular endothelium of the cremaster muscle preparation of Syrian hamsters.<sup>112</sup> A subsequent investigation by Kobayashi and co-workers studied the biodistribution of Gadolinium-functionalized G2–NH<sub>2</sub> to G10–NH<sub>2</sub> conjugates administered intravenously into normal mice.<sup>89</sup> Results showed that Gadolinium-functionalized G2–G4 dendrimers were quickly excreted in urine after 3 min of their intravenous injection whereas G5 and higher generations displayed limited renal secretion because of their larger hydrodynamic volume.<sup>89</sup> These results clearly indicate the influence of dendrimers size/hydrodynamic volume on their transport across the microvascular endothelium in vivo.

Cationic dendrimers show high nonspecific uptake by the RES particularly in the liver and lungs, which reduces their accumulation in tumor tissue.<sup>23,27,52,113–115</sup> Upon comparing the biodistribution of cationic G5–NH<sub>2</sub> dendrimers and their neutral counterparts prepared by partial or full acetylation of the surface amine groups in nude mice bearing melanoma and prostate tumors, results showed that both dendrimers displayed a similar distribution profile to all major organs within 1 h after dendrimers injection with particularly high

accumulation in the lungs, kidneys, and liver (27.9–28.6% ID/g).<sup>114</sup> While the cationic and neutral dendrimers displayed similar biodistribution profiles, cationic dendrimers showed higher net accumulation in each organ due to their favorable electrostatic interaction with the negatively charged epithelial and endothelial cell surface. It is interesting to note that all polylysines,<sup>23,52</sup> anionic PAMAM–COOH dendrimers,<sup>115</sup> and polyester dendrimers<sup>27</sup> exhibit high distribution to the liver and quick elimination into the urine. This biodistribution profile can be attributed to the dendrimer's small hydrodynamic volumes, which results in less than 5% of the initial dose remaining in the systemic circulation 24 h after administration.<sup>27,52</sup>

Attachment of PEG arms to the dendrimer surface increases their size and molecular weight, thus reducing their systemic clearance and improving their biocompatibility.<sup>4,22,23,116</sup> Specifically, attachment of PEG chains with molecular weight up to 20 kDa to the dendrimer's surface groups increases their plasma half-life to 50 h for G3 polyester dendrimers,<sup>4,23</sup> 75.4 h for polylysine dendrimers,<sup>23</sup> and 100 h for triazine dendrimers.<sup>22</sup> Bhadra et al. showed that the attachment of PEG (5 kDa) chains to 25% of the surface groups of G4–NH<sub>2</sub> dendrimers results in a 3-fold reduction in their hemolytic activity compared to the parent dendrimers.<sup>117</sup> Another in vivo study showed that intraperitoneal administration of melamine dendrimers into Swiss–Webster mice induces significant hepatic toxicity at doses  $\geq 10$  mg/kg,<sup>118</sup> whereas PEGylation of 50% of the surface NH<sub>2</sub> groups would enhance its biocompatibility and increase the tolerated dose to 1 g/kg.<sup>119</sup> These studies clearly indicate the positive effect of surface PEGylation of PAMAM dendrimers by enhancing their plasma residence time and reducing their nonspecific toxicity.

## 4.2. Active Targeting of Dendrimers Therapeutics

Active targeting of polymer–drug conjugates to cancer cells is commonly achieved by conjugation of tumor-specific targeting ligands such as vitamins, carbohydrate residues, peptides, or antibodies, which selectively bind to receptors that are expressed on the surface of cancer cells. Binding of these ligands to the receptors displayed on cancer cell surface triggers receptor-mediated endocytosis and internalization of the whole conjugate into cancer cells. Dendrimers-based drug delivery systems exploit similar targeting strategies to bypass the nonspecific uptake by the RES systems and increase their net accumulation in cancer cells.<sup>120,121</sup>

Baker and co-workers have extensively utilized folic acid (FA) as a targeting ligand for their dendrimers-based drug delivery systems.<sup>13,114,121–124</sup> The rationale behind using FA as a targeting ligand is its affinity to folic acid receptors (FAR) overexpressed by human breast, lung, and brain tumors.<sup>121</sup> Attachment of 5 FA ligands per dendrimer appeared to trigger receptor-mediated endocytosis into cancer cells.<sup>125</sup> FA-targeted dendrimers-based drug delivery systems exhibit substantially higher accumulation and toxicity in FAR-positive cancer cells compared to nontargeted dendrimers<sup>122,126</sup> and free anticancer drugs.<sup>14,127</sup> Specifically, 100% of FAR-positive KB nasopharynx cancer cells take up FA-targeted G5–MTX conjugates (G5–FA–MTX) after 30 min of incubation, which is approximately a 20-fold increase in cellular accumulation compared to nontargeted G5–MTX conjugates.<sup>122</sup>

Nontargeted G5–MTX conjugates are less toxic (IC<sub>50</sub>  $\approx$  1.0  $\mu$ M MTX equiv) compared to targeted G5–FA–MTX

conjugates (IC<sub>50</sub>  $\approx$  0.3  $\mu$ M MTX equiv) when incubated for 72 h with FAR-positive KB cells.<sup>126</sup> Incubation of targeted G5–FA–MTX conjugates (150 nM equivalent concentration of MTX) with KB cells for 24 h resulted in a 40% reduction in cell proliferation, while no significant difference was observed in cell proliferation between the nontargeted G5–MTX conjugates and the control.<sup>128</sup> While G5–FA–MTX conjugates were found to be more cytotoxic than G5–MTX conjugates, there was little difference in their therapeutic activity when incubated with FAR-negative cells, which clearly indicates that FA targeting and the associated internalization process is selective for the FAR-positive cancer cells.<sup>126,127</sup>

It is interesting to note that utilizing FA as a targeting agent in the in vitro efficacy studies by Baker's group was believed to limit the overall anticancer activity of the G5–FA–MTX conjugates since MTX exhibits its anticancer activity through an antifolate pathway. This indicates that the FA incorporated in G5–FA–MTX conjugates can effectively “rescue” the FA-deprived cancer cells from the anticancer effects of MTX and act as an apoptosis reversing agent.<sup>122,126</sup> This was later confirmed by in vitro cytotoxicity results of G5–FA–MTX conjugates incubated with FAR-positive cells, which showed a dramatic decrease in conjugate's toxicity in the presence of free FA. Specifically, viability of KB cells treated with the highest concentration of G5–FA–MTX conjugates (225 nM equiv of MTX) went from 50% viability in FA-free medium to 100% viability in the presence of 50  $\mu$ M free FA.<sup>128</sup>

In vivo biodistribution studies of targeted G5–FA conjugates in KB tumor-bearing mice showed a 4-fold increase in their tumor accumulation compared to nontargeted G5 dendrimers 4 days after administration.<sup>121</sup> As a result of this improved tumor localization of targeted conjugates, biweekly doses of G5–FA–MTX conjugates (at MTX equivalent doses of 5.0–7.2 mg/kg) into KB tumor-bearing SCID mice led to survival rates that were roughly 40 days longer than the mice receiving parallel and equal doses of nontargeted G5–MTX conjugates.<sup>121</sup>

Other groups used different targeting agents including peptides to direct dendrimers-based drug delivery systems to cancer-specific receptors. Falciani et al. used neurotensin (NT) peptides to develop NT-targeted dendrimers carrying chlorin e6 (Che6) and MTX chemotherapeutic agents to different malignancies expressing the neurotensin receptor, which include colon, pancreatic, prostate, and small-cell lung carcinomas.<sup>51</sup> Treatment of HT29 tumor-bearing mice with targeted NT–MTX conjugates for 20 days showed reduction in tumor size to approximately one-third the size of the tumors in mice receiving saline, free MTX, or scrambled NT–MTX conjugates at an equal drug concentration, which indicates the therapeutic benefit of the targeting approach.<sup>51</sup> Another example is reported by Hildgen and co-workers, who developed G2 polyether–copolyester (PEPE) dendrimer–MTX inclusion complexes for treatment of brain tumors, which utilized D-glucosamine ligands displayed on the conjugate's surface to target the GLUT-1 transporter highly expressed on the luminal side of the endothelial cells of the blood–brain barrier and glioma cancer cells.<sup>129</sup> In vitro studies showed that targeted PEPE–MTX conjugates exhibited 2–8-fold higher accumulation into glioma cells, which resulted in 2–4.5-fold higher cytotoxicity compared to nontargeted dendrimers.<sup>129</sup> Other targeted dendrimer conjugates utilized tetrameric avidin glycoproteins to target



lectins differentially expressed on the surface of ovarian carcinoma cells.<sup>130</sup> Yet another PAMAM construct utilized J591 antibodies to target the prostate-specific membrane antigen (PSMA), which is a glycoprotein expressed by all prostate cancer cells and supporting vasculature.<sup>131</sup>

Effective targeting of dendrimers-based drug delivery systems requires the choice of a selective ligand and optimization of the ligand valency to tune the binding and dissociation rates of the targeted conjugates to their specific receptor. Baker and co-workers studied the binding kinetics of G5-NH<sub>2</sub> dendrimers displaying cyclic Arg-Gly-Asp (RGD) ligands that selectively target the  $\alpha_v\beta_3$  integrin receptors expressed solely during angiogenesis and thereby present in high numbers in rapidly growing tumor capillaries.<sup>132</sup> Binding of the targeted G5-RGD conjugates to  $\alpha_v\beta_3$  integrin receptors of human umbilical vein endothelial cells was 150 times slower than free RGD, and the associated equilibrium disassociation constant ( $K_D$ ) of the targeted conjugates was 522 times lower compared to that of free RGD.<sup>132</sup> Dijkgraaf et al. studied tumor-specific accumulation of RGD-targeted dendrimers displaying mono-, di-, and tetrameric cyclic RGD ligands in nude mice bearing SK-RC-52 renal carcinoma, which showed that tumor accumulation increased linearly with the increase in the number of RGD ligands ranging from 0.46% ID/g for the monomeric RGD conjugates to 1.52% ID/g for the trimeric ones.<sup>133</sup>

Baker and co-workers carried out a quantitative and systematic analysis of the effect of FA density on the binding of FA-targeted dendrimers to FAR-positive cells.<sup>125</sup> Incubation of G5-NH<sub>2</sub> dendrimers displaying 2.6–13.7 FA ligands per dendrimer with KB cells for 1 h showed that the association constant ( $K_a$ ) increased linearly with the increase in number of FA ligands while the disassociation constant ( $K_D$ ) improved exponentially (2 500 – 166 700 fold) with the increase in FA ligand density compared to free FA. This kinetic profile suggests that targeted dendrimer conjugates are preferentially taken up by targeted cancer cells not as a result of any increase in the endocytic rate but rather due to longer residence times of the conjugates on the cell surface.<sup>125</sup>

## 5. Mechanisms of Drug Loading onto Dendrimer Carriers

### 5.1. Physical Encapsulation of Drug Molecules

The work of Vogtle and co-workers, who looked at entrapment of guest molecules into branched polymers,<sup>1</sup> represents an earlier form of physical encapsulation of poorly soluble drug molecules in dendrimer's voids to improve their aqueous solubility and control their release profile (Figure 13).<sup>24,117,126,134–136</sup> Inclusion of hydrophobic molecules into dendrimers is typically accomplished by simple mixing of the polymer and drug solutions where the hydrophobic drug associates with the nonpolar core through hydrophobic interactions.<sup>24,126,134,135</sup> As a result of this physical interface between the guest molecules and the dendrimer carrier, release of the encapsulated molecules in an aqueous environment is passively controlled by a range of noncovalent interactions including hydrophobic forces, hydrogen bonding, steric hindrance, and electrostatic interactions. To maximize the loading capacity of drug molecules within the dendrimer, one has to carefully consider polymer architecture, specifically the characteristics of the internal voids. Initial computational and experimental studies by Goddard and Tomalia showed that G1–G3  $\beta$ -alanine dendrimers exhibit an oblong



**Figure 13.** Drawing of a dendrimer carrier encapsulating hydrophobic drug molecules in the dendrimer's voids to increase their aqueous solubility and control their release rate.

open structure while G4 and higher generations possess a densely packed surface that is necessary to produce enclosed internal voids that can effectively encapsulate and retain guest molecules.<sup>95,135</sup> Spin-lattice relaxation profiles of acetyl salicylic acid and 2,4-dichlorophenoxy acetic acid encapsulated within a dendritic carrier displayed a decline in carbon-13 relaxation time with increasing dendrimer's generation number from G0.5–G5.5, thus indicating the shielding of the guest molecules in the polymer network. These findings set the stage for development of different inclusion complexes where dendrimers can encapsulate hydrophobic anticancer drugs to improve their aqueous solubility, control their release rates, and achieve cancer therapy.

Kojima et al. reported the encapsulation of DOX and MTX anticancer drugs in PEGylated G3-NH<sub>2</sub> and G4-NH<sub>2</sub> dendrimers with a maximum DOX and MTX encapsulation efficiency of 6.5 mol/mol dendrimer and 25 mol/mol dendrimer, respectively.<sup>134</sup> The encapsulation efficiency of both drugs appeared to increase with the increase in dendrimer's generation number and the increase in the molecular weight of the surface-bound PEG chains from 550 Da to 2 kDa. These results were further supported by another study that compared the *in vitro* and *in vivo* release of 5-fluorouracil (5FU) encapsulated in non-PEGylated G4-NH<sub>2</sub> dendrimers and PEGylated ones displaying 25% capping of the surface groups using 5 kDa PEG chains.<sup>117</sup> The *in vitro* data indicates that the PEGylated dendrimers show 12-fold higher loading capacity and 6-fold slower release of 5FU drug molecules compared to non-PEGylated dendrimers with complete drug release from the PEGylated carriers in 6 days.<sup>117</sup> Furthermore, intravenous administration of PAMAM-5FU complexes (1000  $\mu$ g 5FU equiv) to albino rats showed that the residence time of 5FU in the systemic circulation achieved by the PEGylated complexes was 3 times longer than that for the non-PEGylated derivatives.<sup>117</sup> These results indicate that the attachment of PEG chains to the dendrimer's surface not only slows down the release of the encapsulated drug but also modulates the conformation of the internal voids, thereby improving drug loading efficiency.

Similarly, another study showed that MTX encapsulation into G2 PEPE dendrimers improved when PEG chains (200–400 Da) were present in the internal cavities and increased with the increase in PEG molecular weight.<sup>129</sup> However, attachment of four glucosamine molecules to the

dendrimer's surface decreased the encapsulation of MTX molecules.<sup>129</sup> As expected, PEGylation improved MTX loading (20.3–24.5 mg of MTX/mg of dendrimer) and slowed its release through PEG steric effects, whereas attachment of glucosamine ligands to the dendrimers led to a 10%–15% decline in MTX encapsulation, which is possibly due to folding of the conjugated glucosamine molecules into the dendritic structure, causing congestion of the dendrimer's surface and limiting the penetration of the MTX molecules.

Despite these improvements in the encapsulation and retention of molecules into PEGylated dendrimers, sustained and controlled release of the encapsulated molecules in physiological solutions remains hard to achieve. For example, MTX molecules loaded into PEGylated dendrimers are released 10 times faster in isotonic Tris buffer containing 150 mM NaCl solution compared to nonisotonic Tris buffer.<sup>134</sup> Similarly, Baker and co-workers reported 70% release of the MTX loaded into G5–MTX inclusion complexes upon incubation for 2.5 h in phosphate buffered saline (PBS) compared to insignificant MTX release in water under the same experimental conditions.<sup>126</sup> Grinstaff and co-workers also reported the release of 90% of the anticancer drug 10-hydroxycaptotecin (10HCPT) loaded into G4.5 PGLSA dendrimers upon incubation for 2.5 h in PBS.<sup>24</sup> It is important to note that PEPE–MTX<sup>129</sup> and PGLSA–10HPCT<sup>137</sup> inclusion complexes exhibited 10- and 4-fold higher cytotoxicity against cancer cells compared to equal concentrations of the free drug, respectively. However, this enhanced anticancer activity is simply a result of rapid bolus release of the encapsulated drug due to the interaction of the buffer salts with the dendrimers, thus weakening the ionic forces “holding” the loaded drug, which will happen in vivo upon administration of these inclusion complexes, resulting in premature drug release into the systemic circulation causing nonspecific toxicity.

One approach to control the rate of drug release from the inclusion complexes is to encapsulate them in a liposomal envelope forming modulatory liposomal controlled release systems (MLCRS).<sup>138</sup> DOX was the drug used in this hybrid system where 3.7 mol of DOX were loaded per 1 mol of G4–NH<sub>2</sub> dendrimers. In this study, *N*-tris(hydroxymethyl)-methyl-2-aminoethanesulfonic acid (TES) buffer (pH 7.5) resulted in 96.6% loading of the added DOX compared to 68.9% DOX loading in acetate buffer (pH 4.5), which is possibly due to the limited electrostatic repulsion between the cationic dendrimers and ionized DOX molecules at pH 4.5. Incubation of MLCRS in cell culture medium at 37 °C for 48 h resulted in release of 12% of the loaded DOX, which is a significant improvement compared to the observed rapid drug release with the conventional inclusion complexes. These studies collectively show that loading of therapeutic molecules into different dendrimers depends on dendrimers generation number, internal composition, net surface charge, and type and degree of functionalization of surface groups. These parameters affect the volume of the internal voids and the physical interactions between guest molecules and the dendrimers core, thus controlling the degree of drug loading and the associated release kinetics. Nevertheless, the issue of rapid drug release from dendrimers-based inclusion complexes remains a significant challenge. While liposomal encapsulated complexes seem promising in terms of controlling the release rates of the encapsulated drugs, their activity

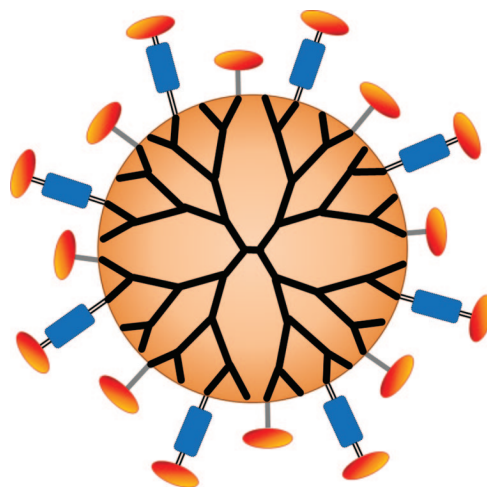


**Figure 14.** Schematic drawing showing a dendrimer–drug conjugate where the drug molecules (red ovals) are either directly coupled (solid lines) to dendrimer's surface groups or via a pH-sensitive linkage (blue rectangle).

against different tumors need to be further evaluated both in vitro and in vivo.

## 5.2. Chemical Conjugation of Drug Molecules

Covalent conjugation of anticancer drugs to dendrimer's surface groups has been used to achieve controlled spatial and temporal release of the attached drugs. The large number of dendrimers' surface groups and the versatility in their chemical structures allow the conjugation of different anticancer drugs, imaging agents, and/or targeting ligands while maintaining the dendrimer's compact spherical geometry in solution (Figure 14).

### 5.2.1. Direct Coupling

In the early 1990s, Barth and co-workers conjugated boronated monoclonal antibodies to a dendrimer carrier via stable urea linkages and utilized this conjugate for neutron capture therapy where localized neutron ionization would cause necrosis of neighboring cancer cells.<sup>113,139</sup> This conjugate achieved high loading capacities of 250–1000 boron atoms per G4 dendrimer while retaining 82% of the antibodies activity in vitro. A few years later, Duncan and co-workers reported the coupling of cisplatin (Pt), a hydrophobic DNA intercalating agent, to G3.5 PAMAM dendrimers via an ester linkage.<sup>140</sup> PAMAM–Pt conjugates carried 20–25 weight % platinum exhibiting 10-fold higher aqueous solubility compared to free Pt and displayed great stability (<1% Pt release) upon incubation in PBS (pH 7.4) and citrate buffers (pH 5.5) at 37 °C for 72 h.<sup>140</sup> Despite the high aqueous solubility and stability of these conjugates, they failed to produce the desired anticancer activity due to limited drug release. Specifically, PAMAM–Pt conjugates displayed insignificant toxicity toward three cancer cells lines when treated with  $0.1 \times 10^{-5}$ –0.01 mg/mL Pt equivalent for 72 h.<sup>140</sup> Similarly, PAMAM–DOX conjugates exhibited 5-fold lower toxicity toward HeLa cells upon incubation with 0.001–1000  $\mu$ M DOX equivalent for 24 h compared to free DOX, which is a result of insignificant drug release (<5% of DOX is released upon incubation in PBS solution for 24 h).<sup>141</sup> These observations were further supported by a separate evaluation of the in vitro and in vivo activity of

amide-linked PAMAM–MTX conjugates where results showed that PAMAM–MTX has 2.7 log units higher  $IC_{50}$  values on glioma cells compared to free MTX *in vitro*, and there was no increase in the survival rate of glioma-bearing rats receiving the PAMAM–MTX conjugates compared to those receiving an equal dose of free MTX.<sup>137</sup> Other classes of therapeutic molecules including Che6 and DOX anticancer drugs,<sup>27,34,51</sup> natural curcumin derivatives,<sup>142</sup> BH3 pro-apoptotic peptide,<sup>127</sup> and photosensitizing agents<sup>120,143</sup> were coupled to a dendritic carrier, which significantly increased the solubility of the loaded drug; however, the associated *in vitro* and *in vivo* anticancer activity markedly decreased due to limited release of the loaded drug.

Studies also showed that the conformation of the anticancer drug molecules displayed on the dendrimer's surface is a critical design parameter for retention of their cytotoxic activity. Gurdag et al. compared the anticancer activity of MTX when coupled through its amine group to the carboxylic acid surface groups of G2.5–COOH dendrimers forming stable amide linkages versus MTX coupling through its carboxylic group to the primary amine groups of G3–NH<sub>2</sub> dendrimers.<sup>107</sup> Results showed that G2.5–MTX conjugates were 3-fold more cytotoxic compared to free MTX toward lymphoblastic leukemia cells, whereas G3–MTX conjugates were 10-fold less toxic than the free MTX. Similarly, Baker and co-workers compared the *in vitro* anticancer activity of G5–OH and G5–NH<sub>2</sub> conjugates with MTX attached via ester and amide linkages, respectively.<sup>122</sup> Incubation of ester-linked G5–MTX conjugates with KB cells at a concentration of 1–100 nM MTX equiv resulted in a 10-fold lower  $IC_{50}$  value compared to amide-linked G5–MTX conjugates, which is a result of faster hydrolysis of the ester linkages and release of the incorporated MTX drug molecules.<sup>122</sup> This data was further supported by Minko's report showing that ester-linked PAMAM–TAX conjugates release 25% of the loaded TAX upon incubation for 24 h in PBS solution and produce a 10-fold decrease in the  $IC_{50}$  value observed upon incubation with human ovarian carcinoma cells for 24 h compared to the free drug.<sup>101</sup>

### 5.2.2. pH-Sensitive Linkages

The desire to achieve cancer cell-specific delivery and release of anticancer drugs motivated the development of dendrimer–drug conjugates with hydrolyzable linkages. Specifically, the sought linkages had to remain intact in the systemic circulation but quickly degrade once internalized into the cancer cell and release the attached drug to produce the desired therapeutic activity. The incorporation of pH-sensitive linkages into dendrimer–drug conjugates seemed to fit the desired criteria as they remain stable in the systemic circulation (pH 7.4) but quickly hydrolyze in acidic environment (pH 5–6) like the endosomes/lysosomes, thus releasing the incorporated drug inside the target cell.<sup>144</sup>

In 2006 Szoka and co-workers reported the synthesis of asymmetric bow-tie polyester G3–G4 dendrimers.<sup>144</sup> DOX was conjugated to the G4 side via either a pH-sensitive hydrazone (hyd) or a carbamate linkage to yield dendrimer–hyd–DOX and dendrimer–DOX conjugates, respectively. Dendrimer–hyd–DOX conjugates were stable at pH 7.4 as indicated by the release of <10% of the incorporated DOX compared to the release of 100% of the attached DOX upon incubation at pH 5.0 for 48 h. Dendrimer–hyd–DOX conjugates were more cytotoxic toward colon carcinoma cells with an  $IC_{50}$  of 1.4  $\mu$ g of DOX/

mL compared to carbamate-linked dendrimer–DOX conjugates with an  $IC_{50}$  of 2.0  $\mu$ g of DOX/mL upon incubation for 72 h.<sup>27,34</sup> In addition, dendrimer–hyd–DOX conjugates displayed a remarkable anticancer activity *in vivo* where a single injection at 20 mg/kg of DOX equiv administered 8 days after tumor implantation resulted in complete tumor regression and 100% survival of the treated animals for 60 days.<sup>34</sup> Subsequent reports confirmed the higher *in vitro* and *in vivo* anticancer activity of dendrimer–hyd–DOX conjugates compared to amide-linked conjugates and the free drug.<sup>141,143</sup> For example, G4–hyd–DOX conjugates ( $IC_{50}$  = 8.7  $\mu$ M) were nearly 7 times more cytotoxic toward HeLa cells compared to G4–amide–DOX conjugates ( $IC_{50}$  = 60.2  $\mu$ M).<sup>141</sup> In addition, G4–hyd–DOX conjugates proved to be equally effective against DOX-sensitive and -resistant cells, whereas free DOX was 58 times less effective in inducing apoptosis in resistant cancer cells.<sup>141</sup>

Fluorescence microscopy studies of Ca9–22 cells separately treated with G4.5–hyd–DOX and G4.5–amide–DOX conjugates revealed that the hydrolysis of the hydrazone linkage allows the liberated DOX molecules to enter the nucleus, whereas G4.5–amide–DOX conjugates fail to release the incorporated drug, thus limiting its access to the nucleus and diminishing its therapeutic activity.<sup>143</sup> It is interesting to note that another study showed that smaller G0–DOX conjugates were able to enter the nucleus regardless of the linkage chemistry.<sup>141</sup>

While these pH-sensitive linkages represent a significant improvement over noncleavable conjugates for intracellular drug delivery of anticancer drugs, they only sense the acidity of the endosomal compartment but fail to differentiate between cancer cells and normal healthy ones. Therefore, further selectivity of drug release from dendrimer conjugates can be achieved by development of novel chemical linkages that are sensitive to cancer-specific markers such as intracellular enzymes. This will allow the release of the incorporated drug only in response to these enzymes, which are solely expressed by cancer cells. Initial studies showed that incubation of 1,3,5-tris(3-aminopropyl)benzene dendrimers displaying specific amino acids on their surface, which include phenylalanine, methionine, aspartic acid, or diaminopropionic acid, with proteolytic enzymes would selectively cleave these amino acids with cleavage rate dependent on the dendrimer's generation number.<sup>145</sup> This initial report suggests the potential of enzyme-sensitive conjugates for cancer cell-specific drug delivery.

## 6. Conclusions

Over the past three decades, dendrimers have evolved from a concept to become a new class of polymers with a unique architecture and versatile chemical structures. Progress in controlled polymerization and synthesis techniques have led to the development of well-controlled dendrimers structures with a large number of surface groups that can be utilized to display a range of biological motifs including peptides, proteins, sugars, and targeting agents while carrying a large therapeutic payload either within the dendrimers voids or on their surface. The high loading capacity of dendrimers renders them highly attractive as carriers for delivery of chemotherapeutic agents into tumor tissue for treatment of cancer. PEGylated and non-PEGylated dendrimers proved to encapsulate hydrophobic drug molecules into the hollow voids of their branching architecture, which enhance the aqueous solubility and stability of the encapsulated drug



molecules. However, controlling the release kinetics of the encapsulated drug remains a challenging task that depends on the hydrophobicity and size of the drug, the generation number of the dendritic carrier, and the type and extent of modification of the dendrimer's surface. Both targeted and nontargeted dendrimer–drug complexes successfully extravasate across tumor's leaky vasculature and accumulate in the cancer tissue. However, targeted dendrimer–drug complexes have the added advantage of selectively binding to the receptors displayed on the surface of cancer cells, which increases their residence time on the cell surface and enhances their internalization kinetics into the cell. The enhanced uptake of dendrimer–drug complexes coupled with the endosomal escape capability of cationic dendrimers result in efficient cytoplasmic delivery of the incorporated drug and remarkably higher anticancer activity. One of the issues that received a reasonable degree of attention, and will most likely continue to evolve in the design of dendrimer–drug complexes, is the nature of the linkage connecting the anticancer drug to the dendritic carrier. Incorporation of pH-sensitive linkers in dendrimer–drug conjugates allowed for specific drug release in the cell endosome; however, it does not discriminate between a normal healthy cell and a cancerous one. We expect that future research will focus on the rational design and synthesis of novel linkers that will be recognized and selectively cleaved by enzymes and other biological molecules present exclusively in the cancer cell to achieve an additional degree of control over the site and rate of anticancer drug release from dendrimer–drug conjugates. An additional area of research that is currently being explored is the development of dendrimers clusters, where several dendrimers are bound together through physical or chemical forces to assemble a multifunctional therapeutic system that incorporates the anticancer drug(s), targeting ligands, and/or imaging agents, which will open the door for combination anticancer therapy along with real time in vivo imaging of the targeted tumor. Despite the promise of dendrimers-based drug delivery systems, their translation into actual cancer therapies with defined dosing regimen is lagging behind. This can be attributed to a combination of factors including the difficulty of synthesizing the proposed systems in large quantities at clinical-grade purity for clinical trials coupled with regulatory hurdles that demand detailed characterization of the polymeric carriers, the linkages, and the incorporated drug. One suspects that the national interest in transferring promising drug delivery systems from the preclinical side to the clinical arena will expedite the evaluation of dendrimers-based drug delivery systems in cancer patients. This is certainly an interesting time for sophisticated dendrimers-based drug delivery systems to emerge as clinically viable anticancer therapies.

## 7. Abbreviations

5FU	5-fluorouracil
10-HCPT	10-hydroxycaptothecine
RGD	arg-glyasp
$K_a$	association rate
CPT	camptothecin
Che6	chlorin e6
Pt	cisplatin
DCC	dicyclohexylcarbodiimide
$K_D$	disassociation rate
DOX	doxorubicin
EPR	enhanced permeability and retention
EDA	ethylenediamine

FA	folic acid
FAR	folic acid receptor
Gal–GalNAc	galactose– <i>N</i> -acetylgalactose
Hyd	hydrazone
HCl	hydrochloric acid
HB	hydroxybutanoic
NHS	<i>N</i> -hydroxysuccinimide
MTX	methotrexate
MLCRS	modulatory liposomal controlled-release system
GlycoNCA	<i>N</i> -carboxyanhydride glycoside
HPMA	<i>N</i> -(2-hydroxypropyl)methacrylamide
NT	neurotensin
TAX	paclitaxel
% ID	percent injected dose
PBS	phosphate buffered saline
P-dendrimer	phosphorus containing dendrimer
PEPE	polyether–copolyester
PETIM	poly(ether imine)
PEG	poly(ethylene glycol)
PGLSA	poly(glycerol–succinic acid)
PAMAM	poly(amidoamine)
PSMA	prostate-specific membrane antigen
RES	reticular endothelial system

## 8. References

- Buhleier, E.; Wehner, W.; Vogtle, F. *Synthesis* **1978**, 155.
- Tomalia, D. A.; Baker, H.; Dewald, J.; Hall, M.; Kallos, G.; Martin, S.; Roeck, J.; Ryder, J.; Smith, P. *Polymer J.* **1985**, 17, 117.
- Tomalia, D. A.; Naylor, A. M.; Goddard, W. A. *Angew. Chem., Int. Ed.* **1990**, 29, 138.
- Gillies, E. R.; Frechet, J. M. J. *Drug Discovery Today* **2005**, 10, 35.
- Boas, U.; Heegaard, P. M. H. *Chem. Soc. Rev.* **2004**, 33, 43.
- Esfand, R.; Tomalia, D. A. *Drug Discovery Today* **2001**, 6, 427.
- Twyman, L. J.; Beezer, A. E.; Esfand, R.; Hardy, M. J.; Mitchell, J. C. *Tetrahedron Lett.* **1999**, 40, 1743.
- Eichman, J. D.; Bielinska, A. U.; Kukowska-Latallo, J. F.; Baker, J. R. *Pharm. Sci. Technol. Today* **2000**, 3, 232.
- Duncan, R.; Izzo, L. *Adv. Drug Delivery Rev.* **2005**, 57, 2215.
- El-Sayed, M.; Ginski, M.; Rhodes, C.; Ghandehari, H. *J. Controlled Release* **2002**, 81, 355.
- Jeyprasesphant, R.; Penny, J.; Jalal, R.; Attwood, D. *Int. J. Pharm.* **2003**, 252, 263.
- Chen, H.-T.; Neerman, M. F.; Parrish, A. R.; Simanek, E. E. *J. Am. Chem. Soc.* **2004**, 126, 10044.
- Majoros, I. J.; Thomas, T. P.; Mehta, C. B.; Baker, J. R. *J. Med. Chem.* **2005**, 48, 5892.
- Majoros, I. J.; Myc, A.; Thomas, T.; Mehta, C. B.; Baker, J. R. *Biomacromolecules* **2006**, 7, 572.
- Luo, D.; Haverstick, K.; Belcheva, N.; Han, E.; Saltzman, W. M. *Macromolecules* **2002**, 35, 3456.
- Sonawane, N. D.; Szoka, F. C.; Verkman, A. S. *J. Biol. Chem.* **2003**, 278, 44826.
- Boussif, O.; Lezoualc'h, F.; Zanta, M. A.; Mergny, M. D.; Scherman, D.; Demeneix, B.; Behr, J. P. *Proc. Natl. Acad. Sci.* **1995**, 92, 7297.
- Krishna, T. R.; Jain, S.; Tatu, U. S.; Jayaraman, N. *Tetrahedron* **2005**, 61, 4281.
- Loup, C.; Zanta, M.-A.; Caminade, A.-M.; Majoral, J.-P.; Meunier, B. *Chem.—Eur. J.* **1999**, 5, 149.
- Patri, A. K.; Majoros, I. J.; Baker, J. R. *Curr. Opin. Chem. Biol.* **2003**, 6, 466.
- Gillies, E. R.; Dy, E.; Frechet, J. M. J.; Szoka, F. C. *Mol. Pharm.* **2005**, 2, 129.
- Lim, J.; Guo, Y.; Rostollan, C. L.; Stanfield, J.; Hsieh, J.-T.; Sun, X.; Simanek, E. E. *Mol. Pharm.* **2008**, 5, 540.
- Kaminskas, L. M.; Boyd, B.; Karellas, P.; Krippner, G. Y.; Lessene, R.; Kelly, B.; Porter, C. J. H. *Mol. Pharm.* **2008**, 5, 449.
- Morgan, M. T.; Nakanishi, Y.; Kroll, D. J.; Griscti, A. P.; Carnahan, M. A.; Wathier, M.; Oberlies, N. H.; Manikumar, G.; Wani, M. C.; Grinstaff, M. W. *Cancer Res.* **2006**, 66, 11913.
- Grinstaff, M. W. *Chem.—Eur. J.* **2002**, 8, 2838.
- Goodwin, A. P.; Lam, S. S.; Frechet, J. M. J. *J. Am. Chem. Soc.* **2007**, 129, 6994.
- Padilla De Jess, O. L.; Ihre, H. R.; Gagne, L.; Frechet, J. M. J.; Szoka, F. C. *Bioconj. Chem.* **2002**, 13, 453.
- Stover, T. C.; Kim, Y. S.; Lowe, T. L.; Kester, M. *Biomaterials* **2008**, 29, 359.
- Galie, K. M.; Mollard, A.; Zharov, I. *Inorg. Chem.* **2006**, 45, 7815.

- (30) Parrott, M. C.; Marchington, E. B.; Valliant, J. F.; Adronov, A. *J. Am. Chem. Soc.* **2005**, *127*, 12081.
- (31) Ou, M.; Wang, X.-L.; Xu, R.; Chang, C.-W.; Bull, D. A.; Kim, S. W. *Bioconj. Chem.* **2008**, *19*, 626.
- (32) Russ, V.; Elfberg, H.; Thoma, C.; Kloeckner, J.; Ogris, M.; Wagner, E. *Gene Ther.* **2008**, *15*, 18.
- (33) Lee, J.-S.; Huh, J.; Ahn, C.-H.; Lee, M.; Park, T. G. *Macromol. Rapid Commun.* **2006**, *27*, 1608.
- (34) Lee, C. C.; Gillies, E. R.; Fox, M. E.; Guillaudeu, S. J.; Frechet, J. M. J.; Dy, E. E.; Szoka, F. C. *Proc. Natl. Acad. Sci.* **2006**, *103*, 16649.
- (35) Ihre, H. R.; Padilla De Jess, O. L.; Szoka, F. C.; Frechet, J. M. J. *Bioconj. Chem.* **2002**, *13*, 433.
- (36) Seebach, D.; Herrmann, G. F.; Lengweiler, U. D.; Bachmann, B. M.; Amrein, W. *Angew. Chem., Int. Ed.* **1996**, *35*, 2795.
- (37) Kohman, R. E.; Zimmerman, S. C. *Chem. Commun.* **2009**, 794.
- (38) Shabat, D. *J. Polym. Sci. [A1]* **2006**, *44*, 1569.
- (39) Newkome, G. R.; Lin, X.; Weis, C. D. *Tetrahedron: Asymmetry* **1991**, *2*, 957.
- (40) Kono, K.; Fukui, T.; Takagishi, T.; Sakurai, S.; Kojima, C. *Polymer* **2008**, *49*, 2832.
- (41) Ranganathan, D.; Kurur, S. *Tetrahedron Lett.* **1997**, *38*, 1265.
- (42) Kim, Y.; Zeng, F.; Zimmerman, S. C. *Chem.—Eur. J.* **1999**, *5*, 2133.
- (43) Kress, J.; Rosner, A.; Hirsch, A. *Chem.—Eur. J.* **2006**, *6*, 247.
- (44) Tam, J. P.; Spetzler, J. C. In *Curr. Protoc. Protein Sci.*; John Wiley & Sons Inc.: Hoboken, NJ, 2001.
- (45) Sadler, K.; Tam, J. P. *Rev. Mol. Biotechnol.* **2002**, *90*, 195.
- (46) Sánchez-Sancho, F.; Pérez-Inestrosa, E.; Suau, R.; Mayorga, C.; Torres, M. J.; Blanca, M. *Bioconj. Chem.* **2002**, *13*, 647.
- (47) Nam, H. Y.; Nam, K.; Hahn, H. J.; Kim, B. H.; Lim, H. J.; Kim, H. J.; Choi, J. S.; Park, J.-S. *Biomaterials* **2008**, *30*, 665.
- (48) Choi, J. S.; Lee, E. J.; Choi, Y. H.; Jeong, Y. J.; Park, J. S. *Bioconj. Chem.* **1999**, *10*, 62.
- (49) Choi, J. S.; Nam, K.; Park, J.-y.; Kim, J.-B.; Lee, J.-K.; Park, J.-s. *J. Controlled Release* **2004**, *99*, 445.
- (50) Yamagata, M.; Kawano, T.; Shiba, K.; Mori, T.; Katayama, Y.; Niidome, T. *Bioorg. Med. Chem.* **2007**, *15*, 526.
- (51) Falciani, C.; Fabbri, M.; Pini, A.; Lozzi, L.; Lelli, B.; Pileri, S.; Brunetti, J.; Bindi, S.; Scali, S.; Bracci, L. *Mol. Cancer Ther.* **2007**, *6*, 2441.
- (52) Okuda, T.; Kawakami, S.; Akimoto, N.; Niidome, T.; Yamashita, F.; Hashida, M. *J. Controlled Release* **2006**, *116*, 330.
- (53) Fuchs, S.; Kapp, T.; Otto, H.; Schoneberg, T.; Franke, P.; Gust, R.; Schluter, A. D. *Chem.—Eur. J.* **2004**, *10*, 1167.
- (54) Mulders, S. J. E.; Brouwer, A. J.; van der Meer, P. G. J.; Liskamp, R. M. J. *Tetrahedron Lett.* **1997**, *38*, 631.
- (55) McGrath, D. V.; Wu, M.-J.; Chaudhry, U. *Tetrahedron Lett.* **1996**, *37*, 6077.
- (56) Tono, Y.; Kojima, C.; Haba, Y.; Takahashi, T.; Harada, A.; Yagi, S.; Kono, K. *Langmuir* **2006**, *22*, 4920.
- (57) Kaneshiro, T. L.; Wang, X.; Lu, Z.-R. *Mol. Pharm.* **2007**, *4*, 759.
- (58) Lee, R. T.; Gabius, H. J.; Lee, Y. C. *Carbohydr. Res.* **1994**, *17*, 269.
- (59) Turnbull, W. B.; Stoddart, J. F. *Rev. Mol. Biotechnol.* **2002**, *90*, 231.
- (60) Aoi, K.; Itoh, K.; Okada, M. *Macromolecules* **1995**, *28*, 5391.
- (61) Aoi, K.; Tsutsumiuchi, K.; Yamamoto, A.; Okada, M. *Tetrahedron* **1997**, *53*, 15415.
- (62) Aoi, K.; Tsutsumiuchi, K.; Yamamoto, A.; Okada, M. *Macromol. Rapid Commun.* **1998**, *19*, 5.
- (63) Lindhorst, T. K.; Kieburg, C. *Angew. Chem., Int. Ed.* **1996**, *35*, 1953.
- (64) Page, D.; Aravind, S.; Roy, R. *Chem. Commun.* **1996**, 1913.
- (65) Ashton, P. R.; Boyd, S. E.; Brown, C. L.; Nepogodiev, S. A.; Meijer, E. W.; Peerlings, H. W. I.; Stoddart, J. F. *Chem.—Eur. J.* **1997**, *3*, 974.
- (66) Jayaraman, N.; Nepogodiev, S. A.; Stoddart, J. F. *Chem.—Eur. J.* **1997**, *3*, 1193.
- (67) Zanini, D.; Roy, R. *J. Org. Chem.* **1996**, *61*, 7348.
- (68) Roy, R.; Zanini, D.; Meunier, S. J.; Romanowska, A. *J. Chem. Soc., Chem. Commun.* **1993**, 1869.
- (69) Ozawa, C.; Katayama, H.; Hojo, H.; Nakahara, Y.; Nakahara, Y. *Org. Lett.* **2008**, *10*, 3531.
- (70) Andre, S.; Pieters, R. J.; Vrasidas, I.; Kaltner, H.; Kuwabara, I.; Liu, F.-T.; Liskamp, R. M. J.; Gabius, H.-J. *ChemBioChem* **2001**, *2*, 822.
- (71) Patri, A. K.; Majoros, I. J.; Baker, J. R. *Curr. Opin. Chem. Biol.* **2002**, *6*, 466.
- (72) Frechet, J. M. J. *Proc. Natl. Acad. Sci.* **2002**, *99*, 4782.
- (73) Newkome, G. R.; Moorefield, C. N.; Baker, G. R.; Saunders, M. J.; Grossman, S. H. *Angew. Chem., Int. Ed.* **1991**, *30*, 1178.
- (74) Mattei, S.; Seiler, P.; Diederich, F.; Gramlich, V. *Helv. Chim. Acta* **1995**, *78*, 1904.
- (75) Liu, M.; Kono, K.; Frechet, J. M. J. *J. Controlled Release* **2000**, *65*, 121.
- (76) Gillies, E. R.; Frechet, J. M. J. *J. Am. Chem. Soc.* **2002**, *124*, 14137.
- (77) Lee, J. W.; Kim, J. H.; Hee Joo Kim, S.; Han, C.; Kim, J. H.; Shin, W. S.; Jin, S.-H. *Bioconj. Chem.* **2007**, *18*, 579.
- (78) Ihre, H.; Padilla De Jess, O. L.; Frechet, J. M. J. *J. Am. Chem. Soc.* **2001**, *123*, 5908.
- (79) Maraval, V.; Pyzowski, J.; Caminade, A.-M.; Majoral, J.-P. *J. Org. Chem.* **2003**, *68*, 6043.
- (80) Launay, N.; Caminade, A.-M.; Lahana, R.; Majoral, J.-P. *Angew. Chem., Int. Ed.* **1994**, *33*, 1589.
- (81) Hawker, C. J.; Frechet, J. M. J. *J. Am. Chem. Soc.* **1990**, *112*, 7638.
- (82) Wooley, K. L.; Hawker, C. J.; Frechet, J. M. J. *J. Am. Chem. Soc.* **1991**, *113*, 4252.
- (83) Kawaguchi, T.; Walker, K. L.; Wilkins, C. L.; Moore, J. S. *J. Am. Chem. Soc.* **1995**, *117*, 2159.
- (84) Kolb, H. C.; Finn, M. G.; Sharpless, K. B. *Angew. Chem., Int. Ed.* **2001**, *40*, 2004.
- (85) Wu, P.; Feldman, A. K.; Nugent, A. K.; Hawker, C. J.; Scheel, A.; Brigitte, V.; Pyun, J.; Frechet, J. M. J.; Sharpless, K. B.; Fokin, V. V. *Angew. Chem., Int. Ed.* **2004**, *43*, 3928.
- (86) Wu, P.; Malkoch, M.; Hunt, J. N.; Vestberg, R.; Kaltgrad, E.; Finn, M. G.; Fokin, V. V.; Sharpless, K. B.; Hawker, C. J. *Chem. Commun.* **2005**, 5775.
- (87) Lee, J. W.; Kim, J. H.; Kim, B.-K.; Kim, J. H.; Shin, W. S.; Jin, S.-H. *Tetrahedron* **2006**, *62*, 9193.
- (88) D'Emanuele, A.; Attwood, D. *Adv. Drug Delivery Rev.* **2005**, *57*, 2147.
- (89) Kobayashi, H.; Brechbiel, M. W. *Adv. Drug Delivery Rev.* **2005**, *57*, 2271.
- (90) Sezaki, H.; Takakura, Y.; Hashida, M. *Adv. Drug Delivery Rev.* **1989**, *3*, 247.
- (91) Singer, J. W.; Bhatt, R.; Tulinsky, J.; Buhler, K. R.; Heasley, E.; Klein, P.; Vries, P. d. *J. Controlled Release* **2001**, *74*, 243.
- (92) Winne, K. D.; Seymour, L. W.; Schacht, E. H. *Eur. J. Pharm. Sci.* **2005**, *24*, 159.
- (93) Shi, X.; Majoros, I. J.; Patri, A. K.; Bi, X.; Islam, M. T.; Desai, A.; Ganser, T. R.; Baker, J. R. *Analyst* **2006**, *131*, 374.
- (94) Myc, A.; Douce, T. B.; Ahuja, N.; Kotlyar, A.; Kukowska-Latallo, J.; Thomas, T. P.; Baker, J. R. *Anticancer Drugs* **2008**, *19*, 143.
- (95) Naylor, A. M.; Goddard, W. A.; Keifer, G. E.; Tomalia, D. A. *J. Am. Chem. Soc.* **1989**, *111*, 2339.
- (96) Lee, C. C.; MacKay, J. A.; Frechet, J. M. J.; Szoka, F. C. *Nat. Biotechnol.* **2005**, *23*, 1517.
- (97) Ooya, T.; Lee, J.; Park, K. *Bioconj. Chem.* **2004**, *15*, 1221.
- (98) Jelinkova, M.; Strohalm, J.; Etrych, T.; Ulbrich, K.; Rihova, B. *Pharm. Res.* **2003**, *20*, 1558.
- (99) Kopecek, J.; Kopecková, P.; Minko, T.; Lu, Z.-R. *Eur. J. Pharm. Biopharm.* **2000**, *50*, 61.
- (100) Minko, T.; Kopeckova, P.; Kopecek, J. *Pharm. Res.* **1999**, *16*, 986.
- (101) Khandare, J. J.; Jayant, S.; Singh, A.; Chandna, P.; Wang, Y.; Vorsa, N.; Minko, T. *Bioconj. Chem.* **2006**, *17*, 1464.
- (102) Greenwald, R. B. *J. Controlled Release* **2001**, *74*, 159.
- (103) Saad, M.; Garbuzenko, O. B.; Ber, E.; Chandna, P.; Khandare, J. J.; Pozharov, V. P.; Minko, T. *J. Controlled Release* **2008**, *130*, 107.
- (104) Svenson, S.; Tomalia, D. A. *Adv. Drug Delivery Rev.* **2005**, *57*, 2106.
- (105) Svenson, S. *Eur. J. Pharm. Biopharm.* **2009**, *71*, 445.
- (106) Nori, A.; Kopecek, J. *Adv. Drug Delivery Rev.* **2005**, *57*, 609.
- (107) Gurdag, S.; Khandare, J.; Stapels, S.; Matherly, L. H.; Kannan, R. M. *Bioconj. Chem.* **2006**, *17*, 275.
- (108) Maeda, H.; Wu, J.; Sawa, T.; Matsumura, Y.; Hori, K. *J. Controlled Release* **2000**, *65*, 271.
- (109) Haag, R.; Kratz, F. *Angew. Chem., Int. Ed.* **2006**, *45*, 1198.
- (110) El-Sayed, M.; Ginski, M.; Rhodes, C. A.; Ghandehari, H. *J. Bioact. Compat. Polym.* **2003**, *18*, 7.
- (111) El-Sayed, M.; Rhodes, C. A.; Ginski, M.; Ghandehari, H. *Int. J. Pharm.* **2003**, *265*, 151.
- (112) El-Sayed, M.; Kiani, M. F.; Naimark, M. D.; Hikal, A. H.; Ghandehari, H. *Pharm. Res.* **2001**, *18*, 23.
- (113) Barth, R. F.; Adams, D. M.; Soloway, A. H.; Alam, F.; Darby, M. V. *Bioconj. Chem.* **1994**, *5*, 58.
- (114) Nigavekar, S. S.; Sung, L. Y.; Llanes, M.; El-Jawahri, A.; Lawrence, T. S.; Becker, C. W.; Balogh, L.; Khan, M. K. *Pharm. Res.* **2004**, *21*, 476.
- (115) Malik, N.; Wiwattanapatapee, R.; Klopsch, R.; Lorenz, K.; Frey, H.; Weener, J. W.; Meijer, E. W.; Paulus, W.; Duncan, R. J. *J. Controlled Release* **2000**, *65*, 133.
- (116) Gajbhiye, V.; Kumar, P. V.; Tekade, R. K.; Jain, N. K. *Curr. Pharm. Des.* **2007**, *13*, 415.
- (117) Bhadra, D.; Bhadra, S.; Jain, S.; Jain, N. K. *Int. J. Pharm.* **2003**, *257*, 111.
- (118) Roberts, J. C.; Bhalgat, M. K.; Zera, R. T. *J. Biomed. Mater. Res.* **1996**, *30*, 53.
- (119) Chen, H.-T.; Neerman, M. F.; Parrish, A. R.; Simanek, E. E. *J. Am. Chem. Soc.* **2004**, *126*, 10044.

- (120) Battah, S.; Balaratnam, S.; Casas, A.; O'Neill, S.; Edwards, C.; Battle, A.; Dobbin, P.; MacRobert, A. J. *Mol. Pharm.* **2007**, *6*, 876.
- (121) Kukowska-Latallo, J. F.; Candido, K. A.; Cao, Z.; Nigavekar, S. S.; Majoros, I. J.; Thomas, T. P.; Balogh, L. P.; Khan, M. K.; Baker, J. R. *Cancer Res.* **2005**, *65*, 5317.
- (122) Quintana, A.; Raczka, E.; Piehler, L.; Lee, I.; Myc, A.; Majoros, I.; Patri, A. K.; Thomas, T.; Mule, J.; Baker, J. R. *Pharm. Res.* **2002**, *19*, 1310.
- (123) Choi, Y.; Thomas, T.; Kotlyar, A.; Islam, M. T.; Baker, J. R. *Chem. Biol.* **2005**, *12*, 35.
- (124) Myc, A.; Majoros, I. J.; Thomas, T. P.; Baker, J. R. *Biomacromolecules* **2007**, *8*, 13.
- (125) Hong, S.; Leroueil, P. R.; Majoros, I. J.; Orr, B. G.; Baker, J. R.; Holl, M. M. B. *Chem. Biol.* **2007**, *14*, 107.
- (126) Patri, A. K.; Kukowska-Latallo, J. F.; Baker, J. R. *Adv. Drug Delivery Rev.* **2005**, *57*, 2203.
- (127) Myc, A.; Patri, A. K.; Baker, J. R. *Biomacromolecules* **2007**, *8*, 2986.
- (128) Thomas, T. P.; Majoros, I. J.; Kotlyar, A.; Kukowska-Latallo, J. F.; Bielinska, A.; Myc, A.; Baker, J. R. *J. Med. Chem.* **2005**, *48*, 3729.
- (129) Dhanikula, R. S.; Argaw, A.; Bouchard, J.-F.; Hildgen, P. *Mol. Pharm.* **2007**, *5*, 105.
- (130) Xu, H.; Regino, C. A. S.; Koyama, Y.; Hama, Y.; Gunn, A. J.; Bernardo, M.; Kobayashi, H.; Choyke, P. L.; Brechbiel, M. W. *Bioconj. Chem.* **2007**, *18*, 1474.
- (131) Patri, A. K.; Myc, A.; Beals, J.; Thomas, T. P.; Bander, N. H.; Baker, J. R. *Bioconj. Chem.* **2004**, *15*, 1174.
- (132) Shukla, R.; Thomas, T. P.; Peters, J.; Kotlyar, A.; Myc, A.; Baker, J. R. *Chem. Commun.* **2005**, 5739.
- (133) Dijkgraaf, I.; Rijnders, A. Y.; Soede, A.; Dechesne, A.; Esse, G. W. v.; Brouwer, A. J.; Corstens, F. H. M.; Boerman, O. C.; Rijkers, D. T. S.; Liskamp, R. M. J. *Org. Biomol. Chem.* **2007**, *5*, 935.
- (134) Kojima, C.; Kono, K.; Maruyama, K.; Takagishi, T. *Bioconj. Chem.* **2000**, *11*, 910.
- (135) Morgan, M. T.; Carnahan, M. A.; Immoos, C. E.; Ribeiro, A. A.; Finkelstein, S.; Lee, S. J.; Grinstaff, M. W. *J. Am. Chem. Soc.* **2003**, *125*, 15485.
- (136) Chauhan, A. S.; Svenson, S.; Reyna, L.; Tomalia, D. *Mater. Matters* **2007**, *2*, 24.
- (137) Wu, G.; Barth, R. F.; Yang, W.; Kawabata, S.; Zhang, L.; Green-Church, K. *Mol. Cancer Ther.* **2006**, *5*, 52.
- (138) Papagiannaros, A.; Dimas, K.; Papaioannou, G. T.; Demetzos, C. *Int. J. Pharm.* **2005**, *302*, 29.
- (139) Alam, F.; Soloway, A. H.; Barth, R. F.; Mafune, N.; Adams, D. M.; Knoth, W. H. *J. Med. Chem.* **1989**, *32*, 2326.
- (140) Malik, N.; Evagorou, E. G.; Duncan, R. *Anticancer Drugs* **1999**, *10*, 767.
- (141) Kono, K.; Kojima, C.; Hayashi, N.; Nishisaka, E.; Kiura, K.; Watarai, S.; Harada, A. *Polymer* **2008**, *29*, 1664.
- (142) Shi, W.; Dolai, S.; Rizk, S.; Hussain, A.; Tariq, H.; Averick, S.; L'Amoreaux, W.; Idrissi, A. E.; Banerjee, P.; Raja, K. *Org. Lett.* **2007**, *9*, 5461.
- (143) Lai, P.-S.; Lou, P.-J.; Peng, C.-L.; Pai, C.-L.; Yen, W.-N.; Huang, M.-Y.; Young, T.-H.; Shieh, M.-J. *J. Controlled Release* **2007**, *122*, 39.
- (144) Rihova, B.; Etrych, T.; Pechar, M.; Jelinkova, M.; Stastny, M.; Hovorka, O.; Kova, M.; Ulbrich, K. *J. Controlled Release* **2001**, *74*, 225.
- (145) Kapp, T.; Francke, P.; Gust, R. *ChemMedChem* **2008**, *3*, 635.

CR900174J